THE EFFECT OF FRACTURE CLOSURE ON ECONOMIC VIABILITY OF THE WOLFCAMP – A CASE STUDY

A Thesis

by

STAVROS ANDRONIKOS DEMARCHOS

Submitted to the Office of Graduate and Professional Studies of
Texas A&M University
in partial fulfillment of the requirements for the degree of

MASTER OF SCIENCE

Chair of Committee,	John Killough
Committee Members,	Eduardo Gildin
	Maria Barrufet
Head of Department,	Duane McVay

May 2018

Major Subject: Petroleum Engineering

ABSTRACT

This report is composed of the petrophysical and seismic interpretation and evaluation of a well in the Permian Basin and the effect of fracture closure on economic viability. The research determined the economic viability of the Wolfcamp based upon the various proppant fracture conductivity tables. The shale plays that the report focuses on are the Wolfcamp Shales in the aforementioned basin. These shales are divided into Wolfcamp A, Wolfcamp B, and Wolfcamp C. The Wolfcamp B shale deposit is the best reservoir quality interval. In this study, the petrophysical properties of the reservoir were found through core data, log data, pressure data, and seismic data. Simulations were conducted using the defined extent of the reservoir to observe a history match of the pressure and production for observed well. Furthermore, an analogous well was created to examine the effect of economic viability by using different fracture conductivity tables. The differing scenarios were conducted to emphasize the importance of reliable measurements of geomechanical properties and associated modeling. In this case study, the geomechanical property emphasized is the fracture conductivity with respect to individual proppants. This report will cover the process, methodology, conclusions and recommendations made throughout the Wolfcamp Shale analysis.

CONTRIBUTORS AND FUNDING SOURCES

This work was supervised by a dissertation committee consisting of Professor John Killough [advisor] and Professor Eduardo Gildin of the Department of Petroleum Engineering and Professor Maria Barrufet of the Department of Chemical Engineering. All work for the dissertation was completed independently by the student. There are no outside funding contributions to acknowledge related to the research and compilation of this document.

NOMENCLATURE

V_{sh}	shale volume
GR	gamma ray reading from log
GR_{clean}	minimum gamma ray value
GR_{shale}	maximum gamma ray value
V_{sh_ST}	Steiber model for shale volume
$\emptyset_{D,ss}$	density porosity in water-filled sandstone units
ρ_{bulk}	bulk density
ρ_{ss}	density of sandstone determined from lithology cross-plot
$\emptyset_D^{sh}$	density porosity corrected for shale
$\emptyset_D$	density porosity reading from log
$\emptyset_{D,sh}$	density porosity reading from log in pure shale zone
$\emptyset_N^{sh}$	neutron porosity corrected for shale
$\emptyset_{N,sh}$	neutron porosity reading from log in pure shale zone
$\emptyset_N$	neutron porosity reading from log
$\emptyset_{sh}$	shale porosity
ρ_{sh}	matrix density of shale
$\emptyset_T$	total porosity
F	formation resistivity factor
a	tortuosity
HCPV	hydrocarbon pore volume

m	cementation exponent
n	saturation exponent
OOIP	original oil in place
S_{wt}	total water saturation
S_{wb}	clay bound water saturation
R_w	water resistivity
R_{wb}	clay bound water resistivity
R_t	true water resistivity

TABLE OF CONTENTS

Page

Page

LIST OF FIGURES

Page

Page

Page

LIST OF TABLES

Page

1. INTRODUCTION

As mentioned, this report is composed of the petrophysical and seismic interpretation and evaluation of a well in the Permian Basin and the effect of fracture closure on economic viability. The closest study in regards to the research conducted consists purely of the general comparison of different proppant conductivity tables (Barree et al., 2016). This study is unique and takes the research two steps further than the similar research. First by creating production data for a specific well using the different proppant conductivity tables and second by evaluating the economic viability of the well via proppant fracture conductivity tables. In this study, the petrophysical properties of the reservoir located within the Permian were found through core data, log data, pressure data, and seismic data (Walls et al., 2016). The Permian Basin is located in the western part of Texas and partially located in southeast New Mexico and is divided into the Wolfcamp A, Wolfcamp B, and Wolfcamp C shale layers (Schwartz et al., 2015). The Permian Basin was named for the thick deposit of rock originating from the Permian geologic time period and is bound by Strawn/Devonian/Ellenburger high-side fault closures and a Devonian/Ellenburger sub-thrust structure (Gupta et al., 2017). The Permian is actually composed of smaller basins knowns as the Midland, Delaware and Marfa Basins. The Wolfcamp formation, for which this study covers, is a formation within the Delaware Basin and was created between 299 and 280 million years ago. A unique feature to this reservoir is that the Wolfcamp formation is located within two of the component basins. The Wolfcamp is also located within the Midland Basin; however, this study is only relevant for the Delaware Basin Wolfcamp formation. Respectively, the Delaware Basin is located within the western region of the Permian and the Midland Basin located within the eastern region of the Permian. It is important to note

this difference because the two formations may be referred to as the Wolfcamp, they exhibit different reservoir characteristics.

2. RESERVOIR CHARACTERIZATION

2.1 Gross Interval Thickness

The total unit thickness in Wolfcamp varies from 200 to 600 ft (**Fig. 1**). The total shale layers are comprised of the Wolfcamp A (WA), Wolfcamp B (WB), and Wolfcamp C (WC) shales. The WA shale thickness ranges from 40 to 200 ft (**Fig. 2**). The WB shale thickness ranges from 60 to 400 ft (**Fig. 3**). Lastly, the WC shale thickness ranges from 30 to 120 ft (**Fig. 4**). The WB flow unit is much thicker than the other two layers and is the primary producing zone. Some wells in the Wolfcamp do not have a WA or WB shale layer (Schwartz et al., 2015).

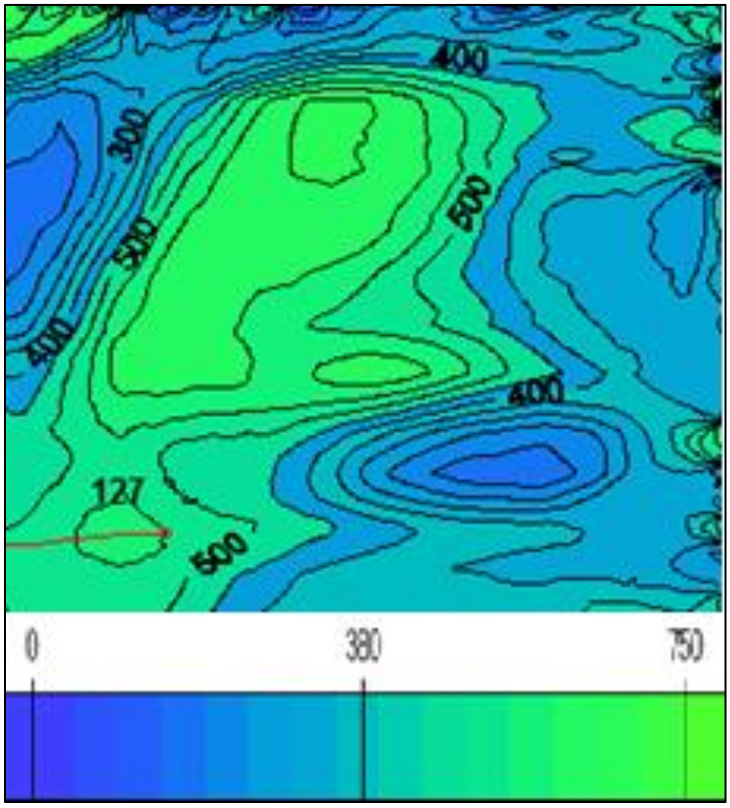

Figure 1: Total Wolfcamp Isopach Map, C.I. =50 ft

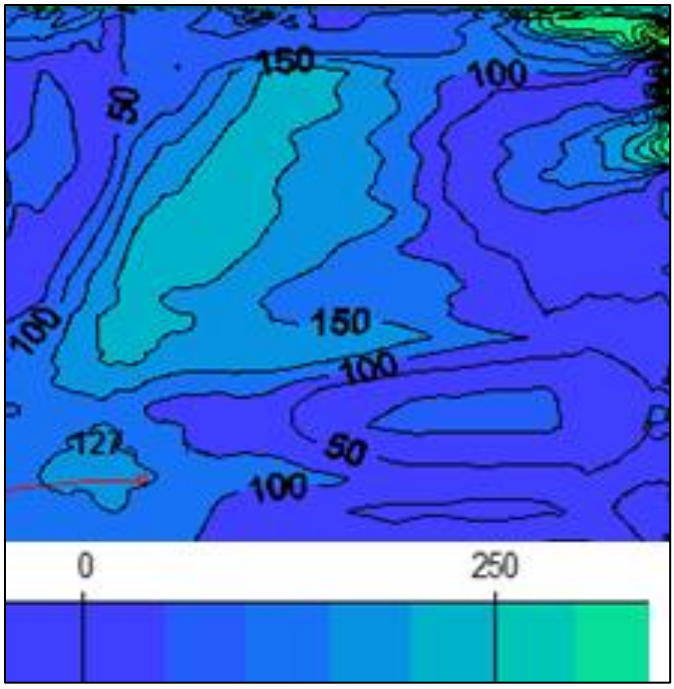

Figure 2: WA Isopach Map, C.I. =50 ft

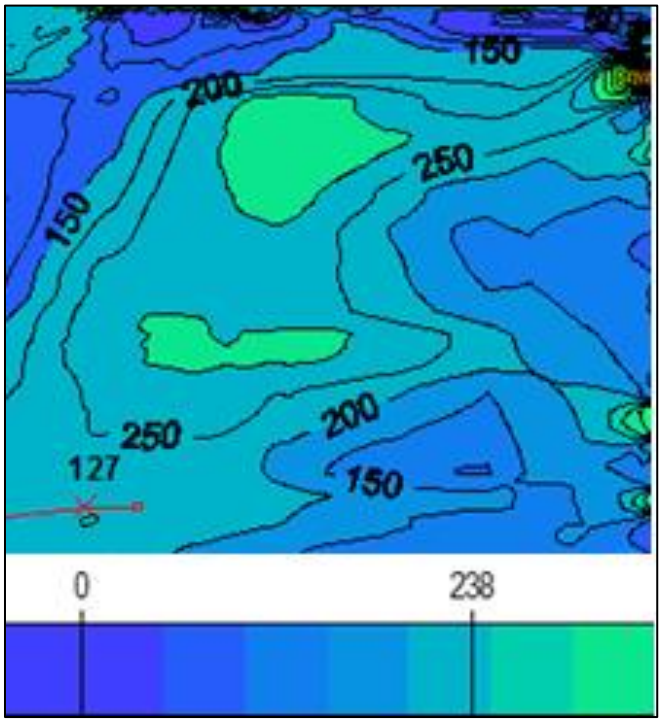

Figure 3: WB Isopach Map, C.I. =50 ft

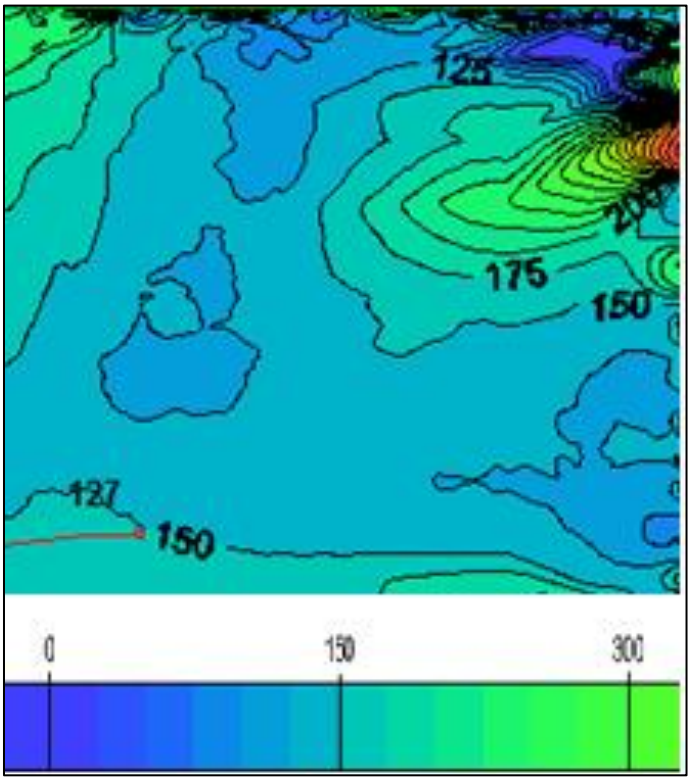

Figure 4: WC Isopach Map, C.I. =50 ft

2.2 Stratigraphic Analysis

The stratigraphic strike cross section shales gradually thin and the WC shale pinches out to the northeast (**Fig. 5**). The WB sand is the thickest flow unit. The strike direction trends from the northwest to the southeast (Kvale and Rahman, 2016).

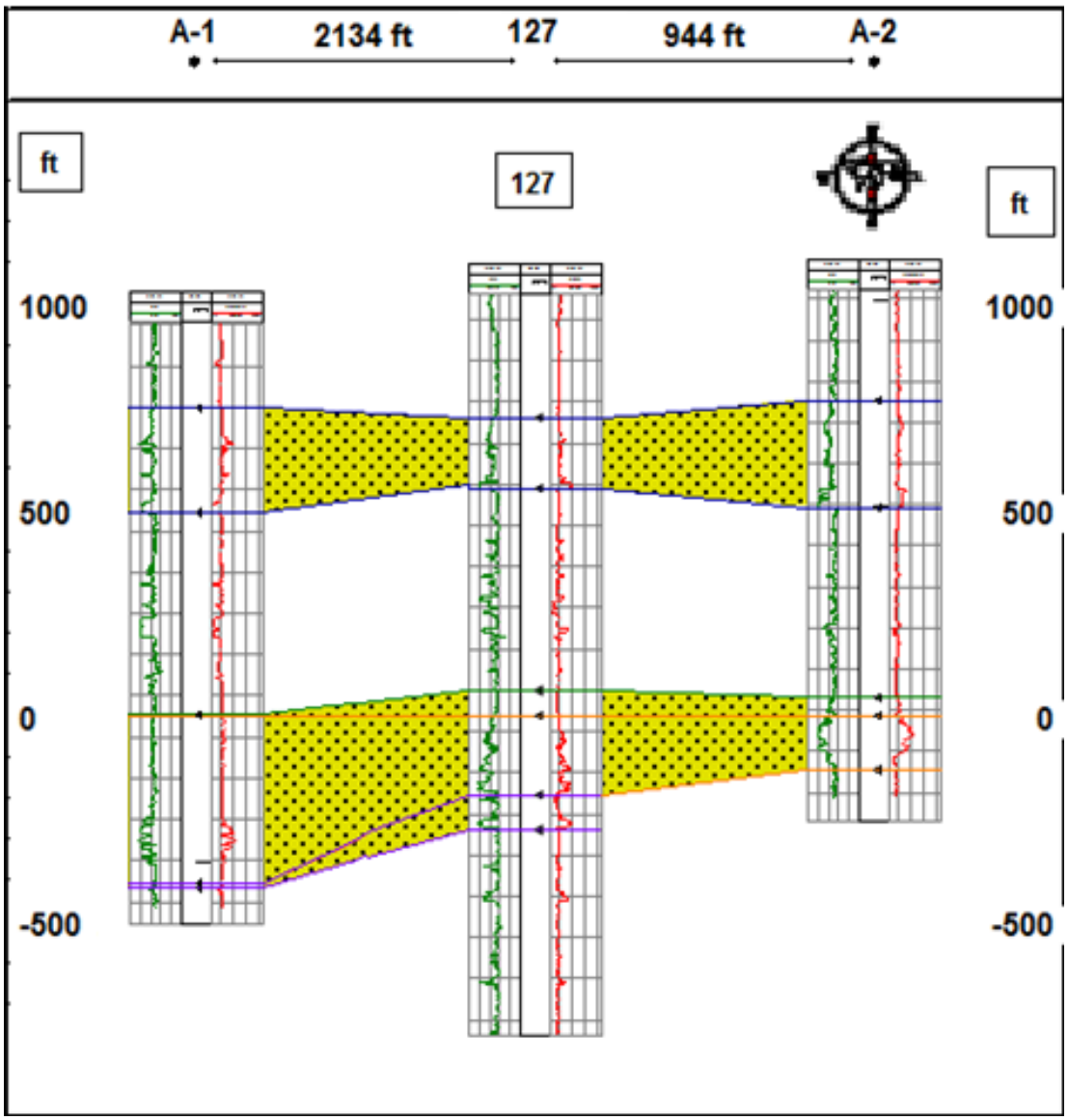

Figure 5: Stratigraphic Cross-Section, Datum: WB Top

2.3 Structural Analysis

There is one fault occurring through the strike, acting as a structural boundary for the shales (**Fig. 6**). An anticline serves as a trap for oil accumulation (Kvale and Rahman, 2016). The reverse fault, located between wells 127 and A-2 created an offset of approximately 50 ft. The

oil-water-contact for the Wolfcamp shales is determined to be located at around a depth of 13,300 ft based on the low resistivity.

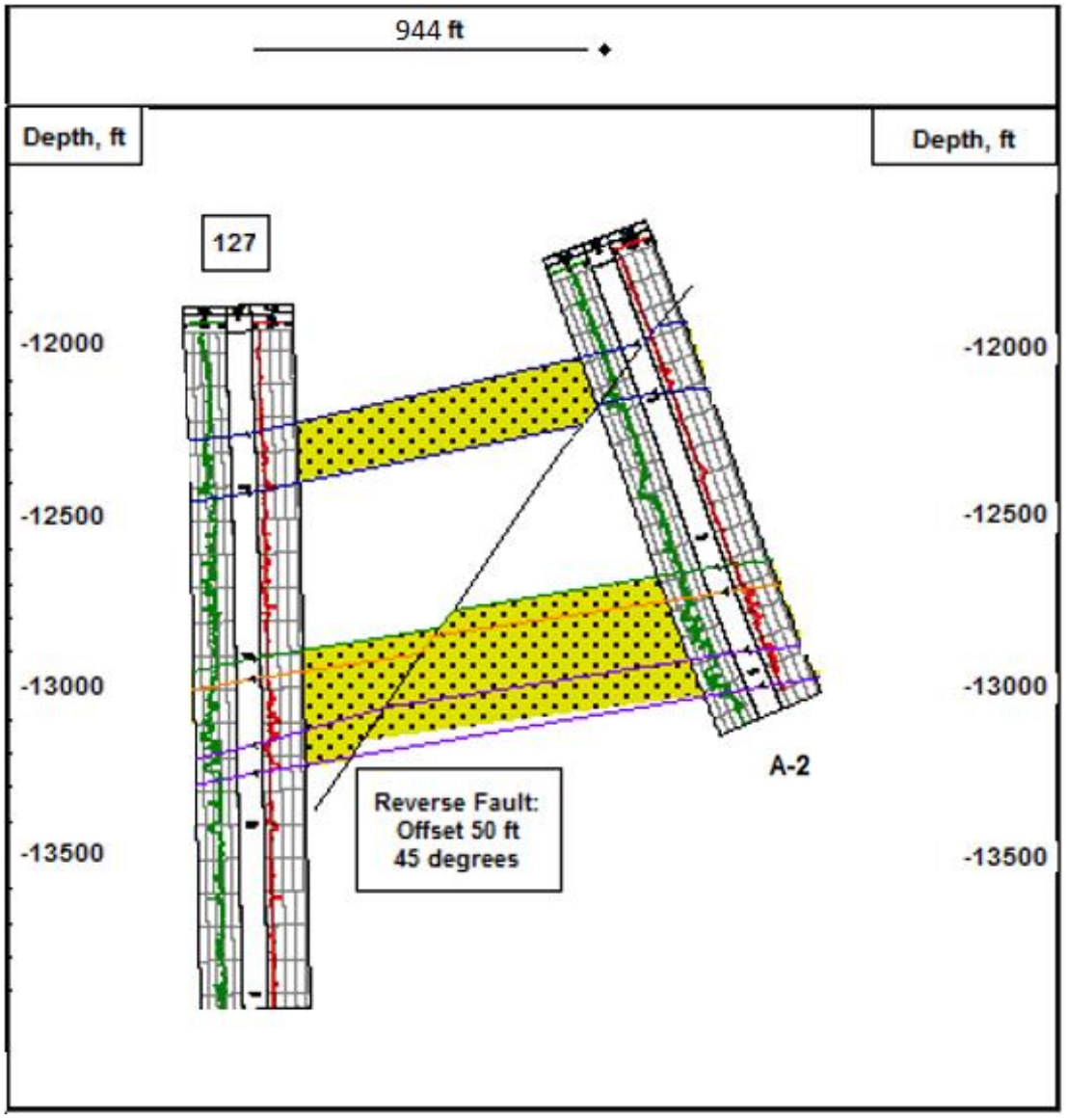

Figure 6: Structural Strike Cross Section, Datum: WA Top

Faults to the north of the field serve as structural boundaries for the Wolfcamp shales. Well logs provide reservoir properties that are a reliable estimate within the well control area

(Pioneer Natural Resource Co., 2016). As the distance from the wellbore increases so does the uncertainty of the values of specific reservoir properties. Well attributes were used to help reduce this uncertainty and provide more accurate property estimations. This was done using correlations between a specific well attributes and reservoir properties. Net-to-gross sandstone ratio, average net sandstone porosity, and average net sandstone permeability were the reservoir properties that were correlated for each Wolfcamp shale interval. Water saturation, porosity, and shale volumes cutoffs that were determined from the petrophysical analysis were used to define these parameters within the well control. Examination of net-to-gross ratio maps of intervals WA, WB, and WC (**Figs. 7**, **8**, and **9**, respectively) shows the highest ratios are located near the crest of the offset within the central fault block of the Wolfcamp. Trends in the net-to-gross ratio decrease further down the slope of the channel (Walls et al., 2016).

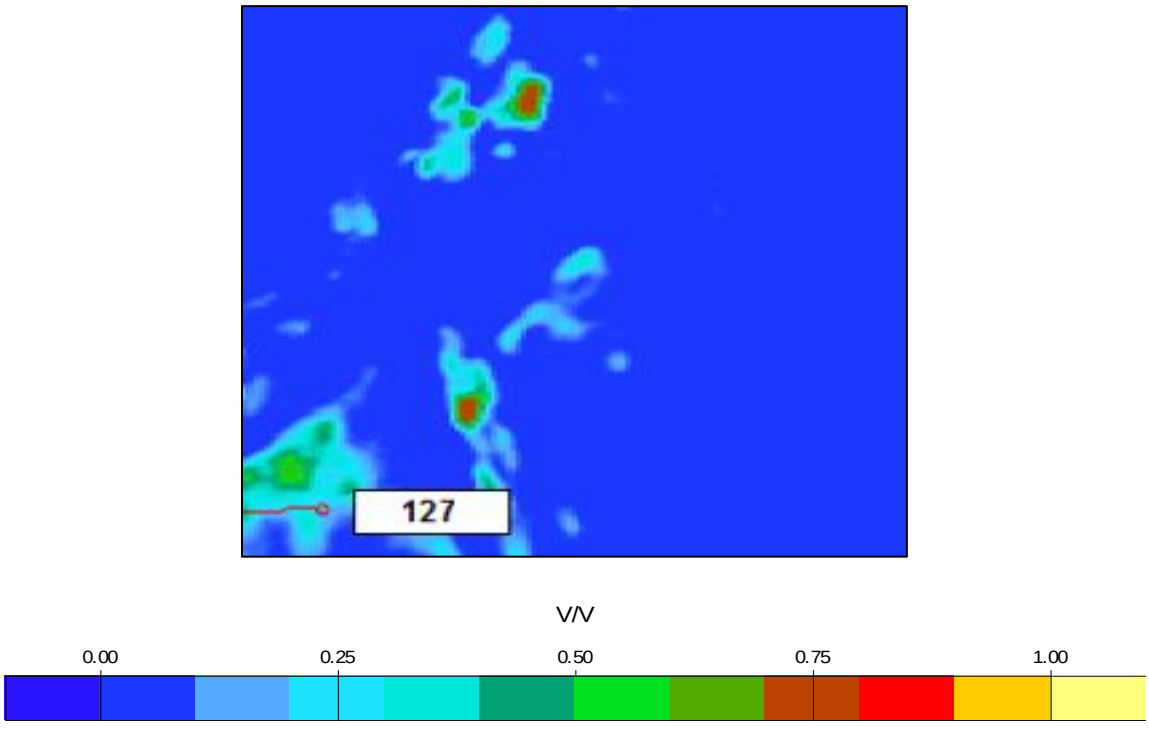

Figure 7: Net-To-Gross Ratio Map of WA Layer

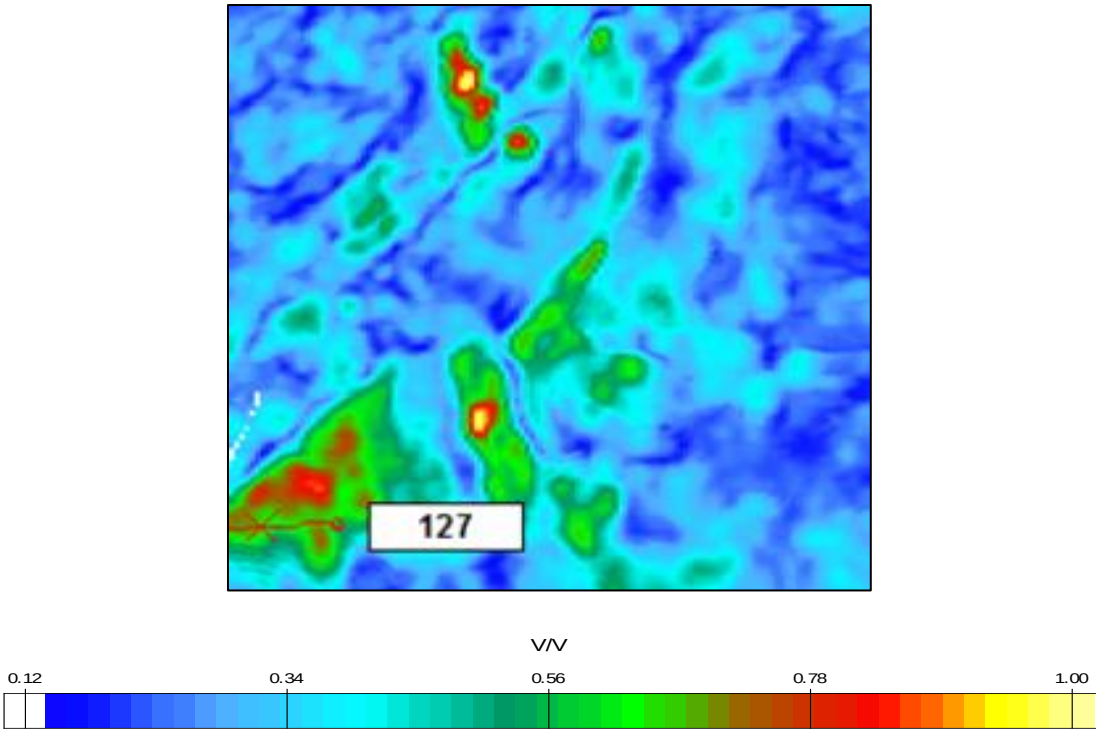

Figure 8: Net-To-Gross Ratio of WB Layer

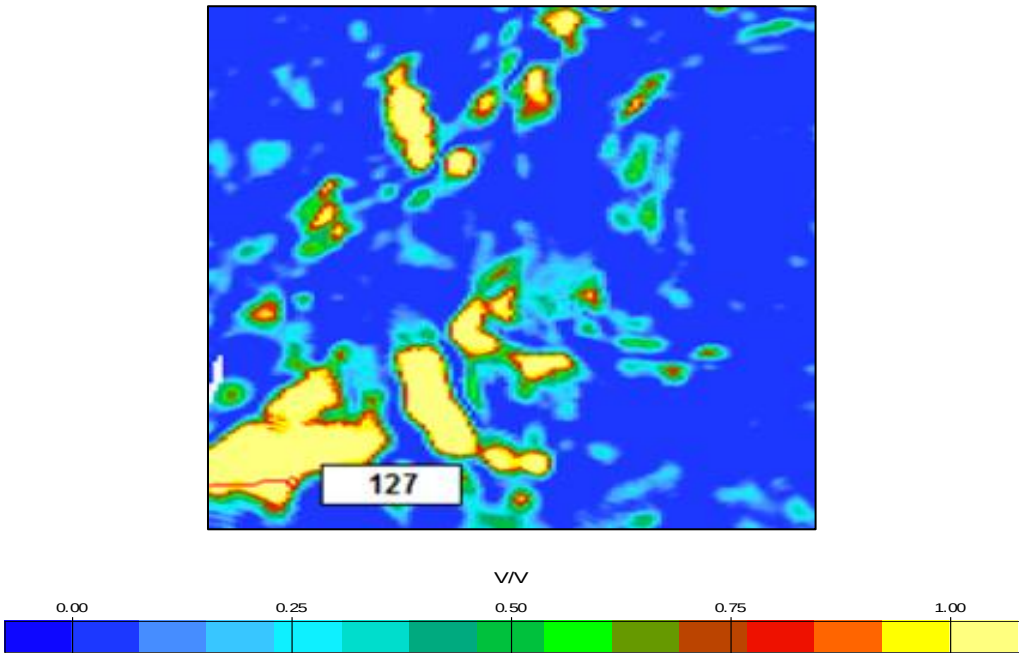

Figure 9: Net-To-Gross ratio of WC Layer

The highest average net shale porosities are present in the same regions of the reservoir as the highest net-to-gross shale ratios. Additionally, the highest average net shale permeability is seen in the same regions. The WA shale had the lowest average net porosity (**Fig. 10**) as well as average net permeability (**Fig. 11**) of all the Wolfcamp shale intervals. The WC shales had the highest average net porosity (**Fig. 12**) as well as the largest average net permeability (**Fig. 13**) of all the flow units within the Wolfcamp shales (Walls et al., 2016). The average net porosity and permeability for the WB shales are featured in **Figs. 14** and **15**, respectively.

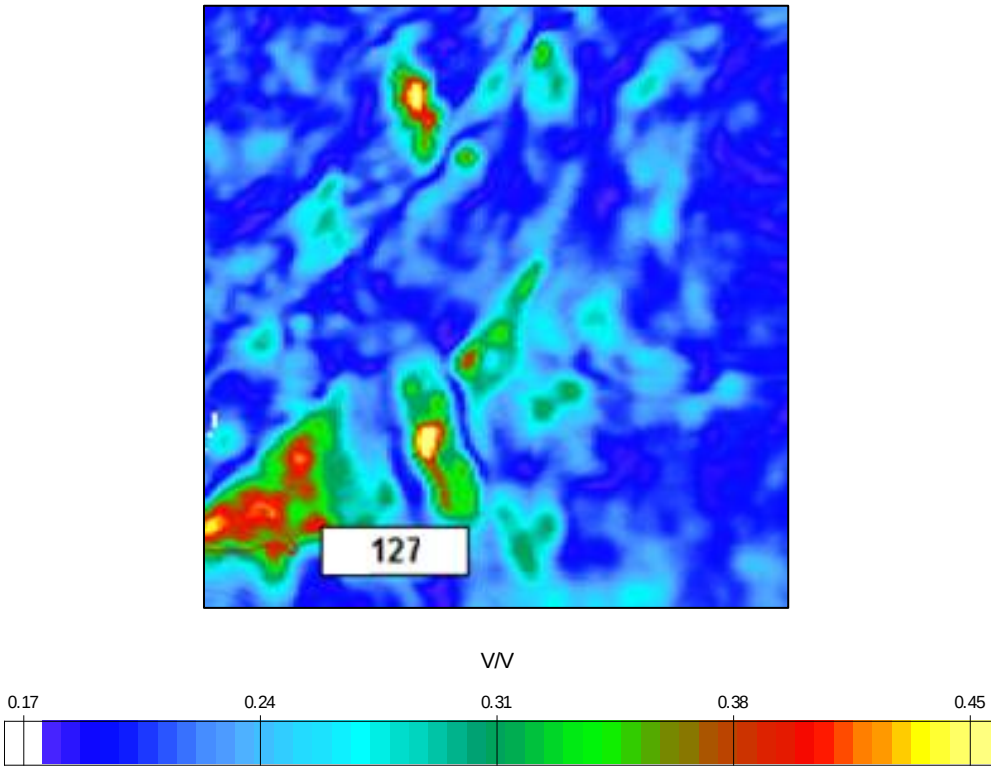

Figure 10: Average Net Porosity for WA Layer

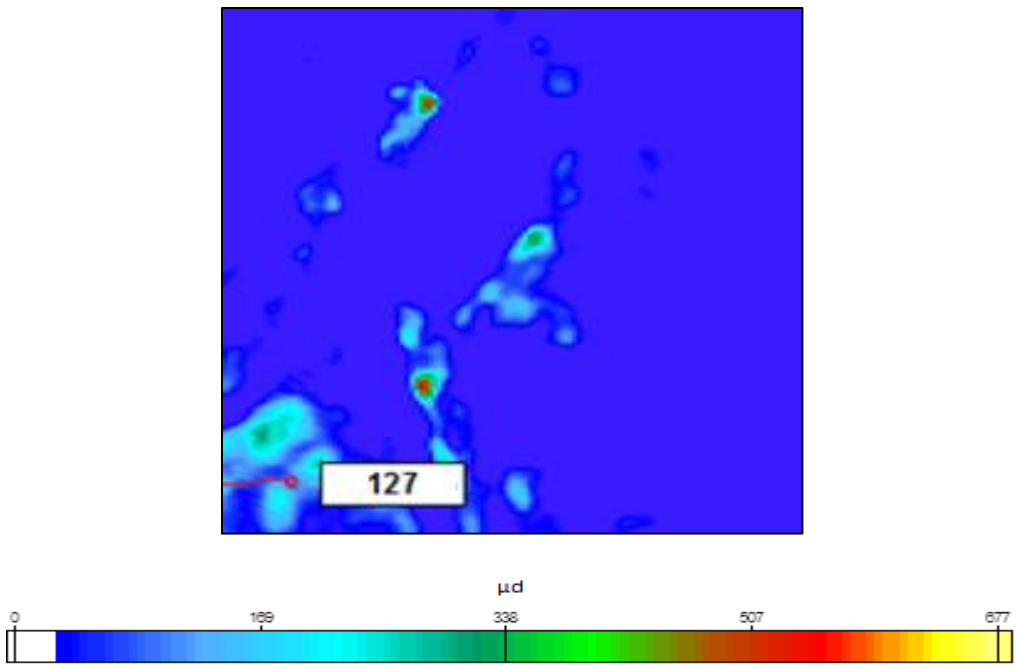

Figure 11: Average Net Permeability for WA Layer

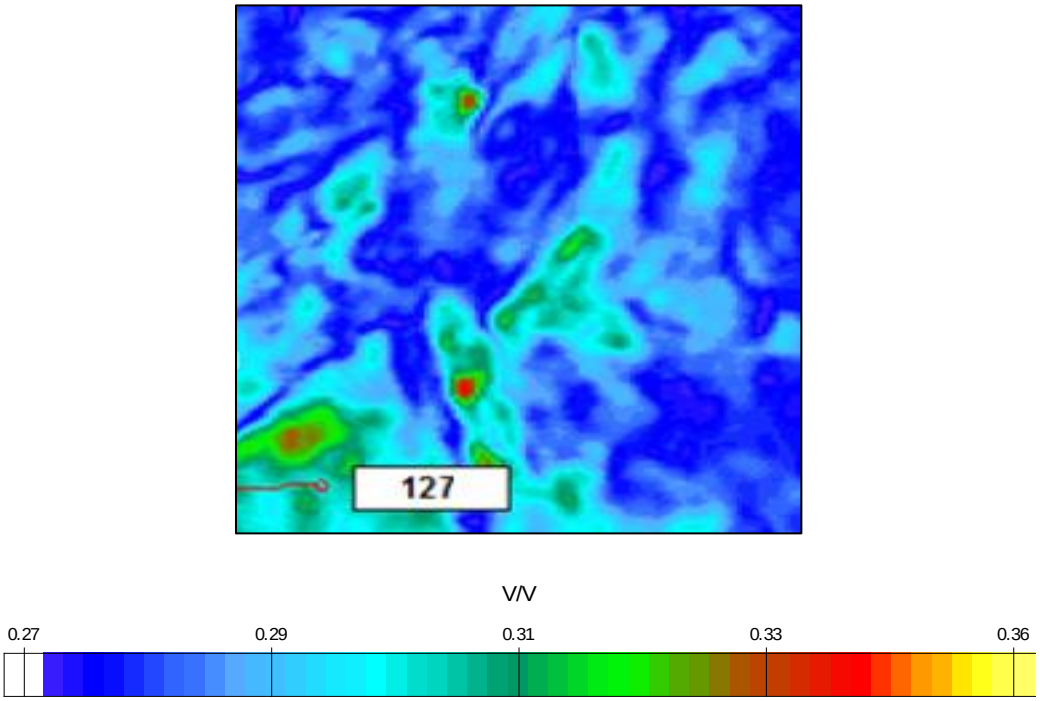

Figure 12: Average net Porosity for WC Layer

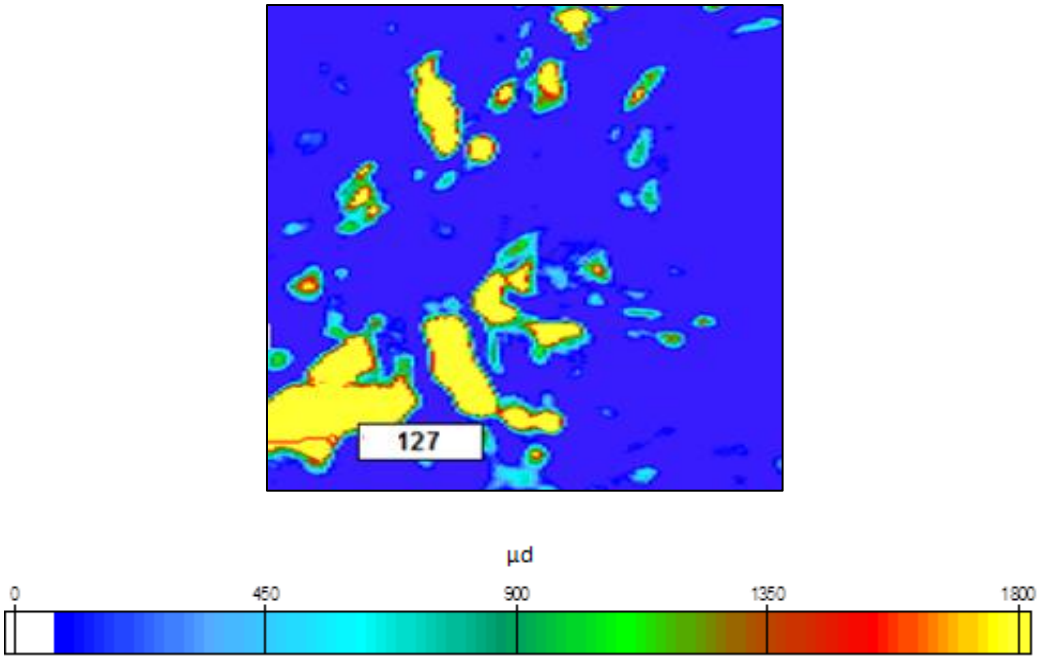

Figure 13: Average Net Permeability for WC Layer

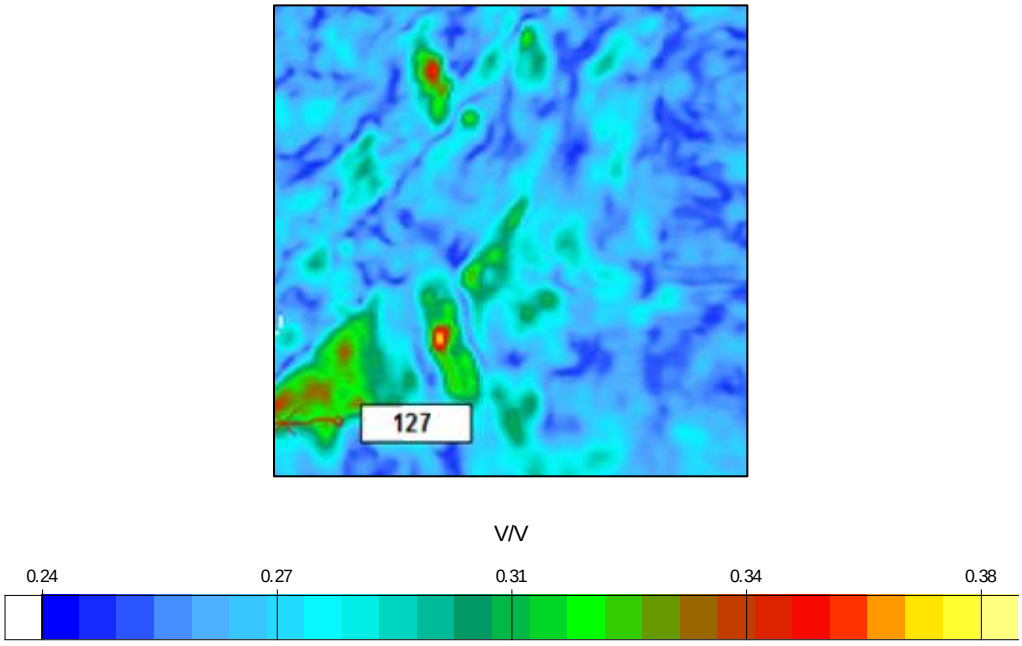

Figure 14: Average Net Porosity for WB Layer

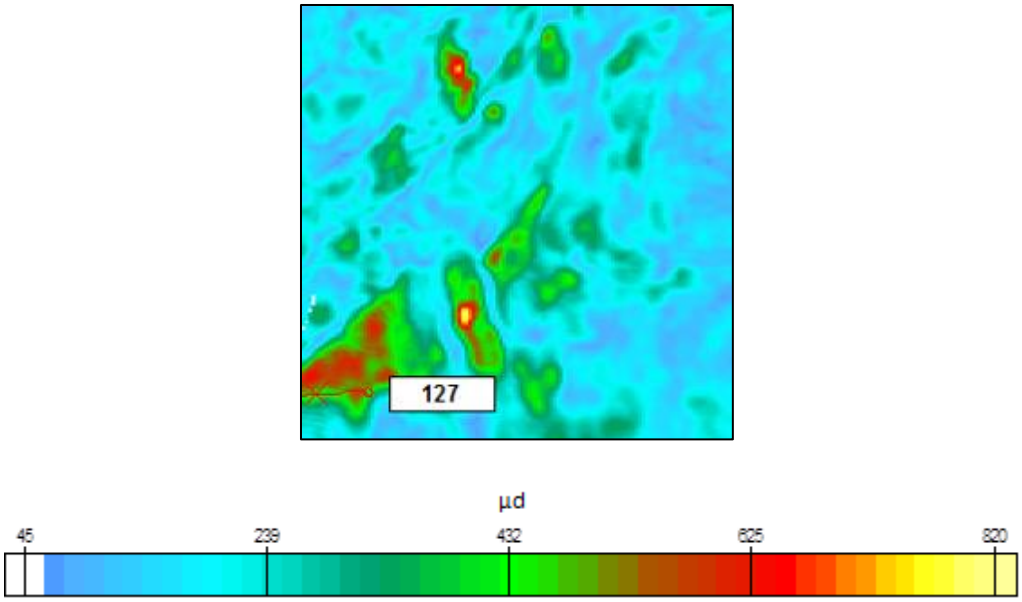

Figure 15: Average Net Permeability for WB Layer

2.4 Total Pore Volume

Total pore volume was estimated for the area of the Wolfcamp shale interval used in this project by first creating a map (**Fig. 16**) that displays the areal extent of the Wolfcamp formation that lies above the OWC within the Wolfcamp shale interval. This map was constructed from the Wolfcamp shale gross thickness, Wolfcamp shale net thickness, Wolfcamp shale average net porosity, and the WA top structure map (Pioneer Natural Resources Co., 2016). The portion of the map that has a color fill of red defines the area above the OWC while everything below the OWC has a color fill of blue. The reservoir's estimated areal extent above the OWC was enclosed within a polygon on Figure 16. The volume and area statistics tool within GeoAtlas was used to calculate the total area within this polygon and resulted in a reservoir area of about 834 acres with a total volume of 61.3 MMbbl. The average water saturation for the Wolfcamp shale was determined using the curve data statistics tool within PRIZM to be 47 percent. The

hydrocarbon pore volume was then determined by multiplying the total volume above the OWC by the average oil saturation (one minus the average water saturation) which yielded 32.5 MMbbls. Using an oil formation volume factor 1.4 bbl/STB from PVT analysis yields an original oil in place (OOIP) estimate of 23.2 MMSTB and is correlative to "Petrophysical Characterization of the Pore Space in Permian Wolfcamp Rocks" (Rafatian and Capsan, 2015). It is important to note that this is just the OOIP of a small area of the Wolfcamp formation, not the entirety.

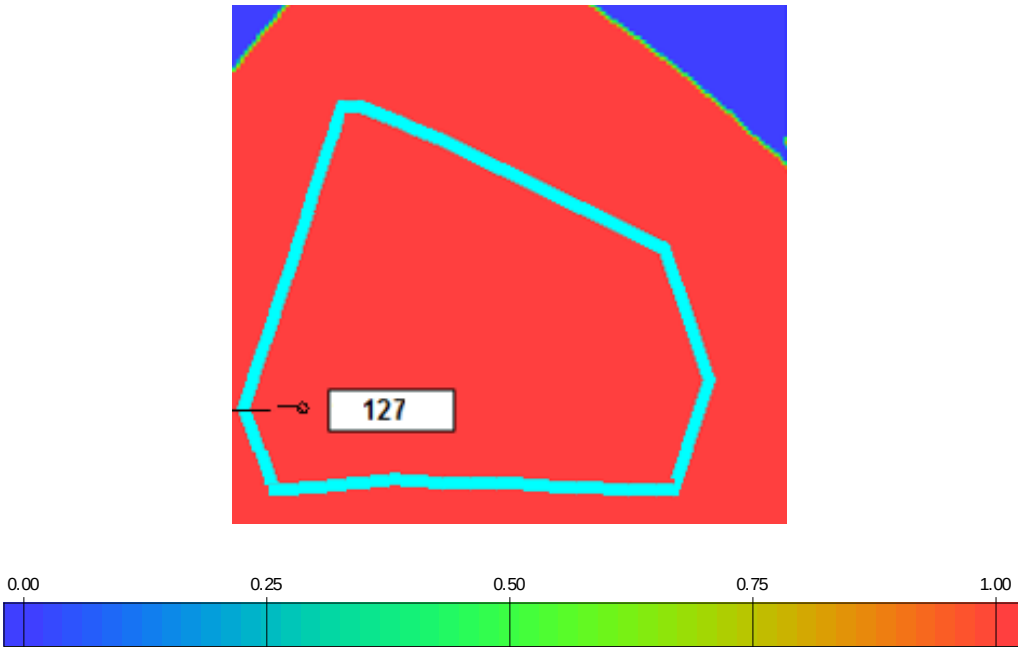

Figure 16: Areal Extent of Wolfcamp Above OWC

3. PETROPHYSICAL EVALUATION

3.1 Introduction

The objectives of the petrophysical analysis were to determine values for porosity, permeability, water saturation, and shale volume for the Wolfcamp formation. From this, the determination of appropriate cut-offs to apply in the hydrocarbon volume and net shale calculation. In order to conduct this study, the available conventional and sidewall core data with the log data provided was integrated. Log data was provided for the wells in the Wolfcamp (Pioneer Natural Resources Co., 2016) and one was selected for the study, however, other local well logs were used to correlate formation data. The log data used in the analysis included gamma ray, resistivity, bulk density, and neutron porosity (Pioneer Natural Resources Co., 2016). Additionally, the log data and the SCAL (Special Core Analysis Laboratories) data were also used to calibrate the petrophysical calculations (Pioneer Natural Resources Co., 2016). Currently, it is mainly being produced by Pioneer Resources and is a relatively young field.

3.2 Data Preparation

The log data provided was already normalized and corrected for environmental effects such as mud-filtrate invasion, tool stand-off, pressure and temperature effects, and salinity effects. Due to the integration of core data, a depth shift of the core data was required to match the depth at which the log data was recorded. **Fig. 17** shows an example for well 127, which required depth shifting of approximately 15 ft (Pioneer Natural Resources Co., 2016).

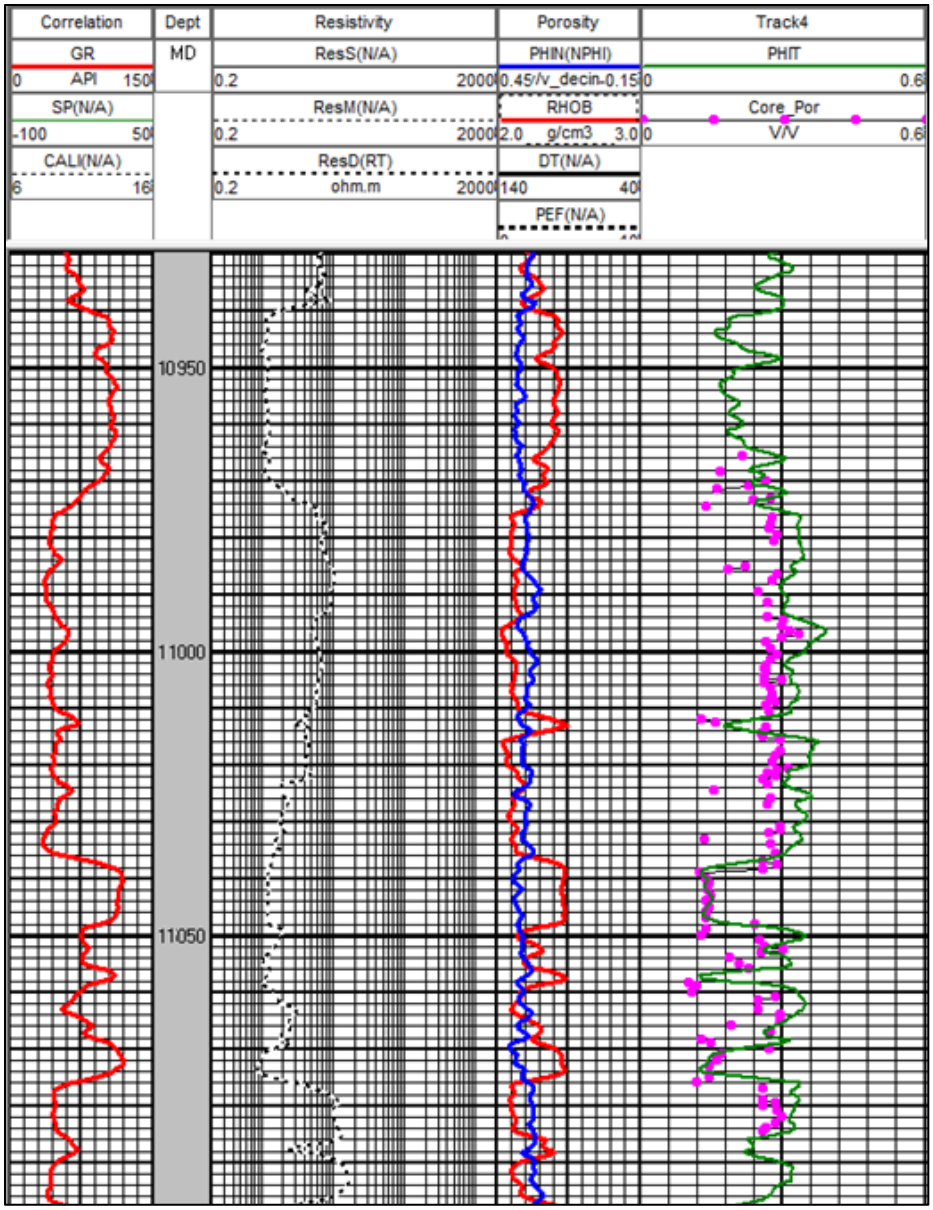

Figure 17: Depth Shifting of Well 127

3.3 Lithology Determination

The main tool in evaluating the lithology was the crossplot of bulk density versus neutron porosity and evaluation steps (Kvale and Rahman, 2016). The Baker Atlas 2446 Salts overlay was used in GeoGraphix to determine the lithology. Techlog was used in the lithology

determination in order to disregard any depths where the shale effect would shift data points to the lower right. The higher GR, indicating more shale, will show up as warmer colors on the Techlog crossplots. The conclusion is that the lithology of the main reservoir is primarily shale with sandstone deposits. **Figs. 18** and **19** demonstrate an example of the process followed to determine the lithology of each reservoir. Figure 18 is a crossplot of bulk density vs. neutron porosity for well 127 in the WB shale interval, since this is the main zone of interest. Just by looking at this figure, it appears that the WB lithology may be leaning more towards dolomite. By looking at Figure 19, it becomes clear the shale is present. Both of the plots contain the same data points, but Figure 19 contains an added color scale for gamma ray data. Because of the high GR readings that may be observed in nearly all of the lower points, this confirms that the Wolfcamp B layer is shale. The primary lithology is shale with a matrix density of 2.68 g/cc. This was determined by drawing a line straight through the remaining points after removing necessary points and reading off the density. This process may be observed in Fig. 28. The core analysis grain density ranges from 2.641 g/cc to 2.813 g/cc which confirm that the value 2.68 g/cc is accurate.

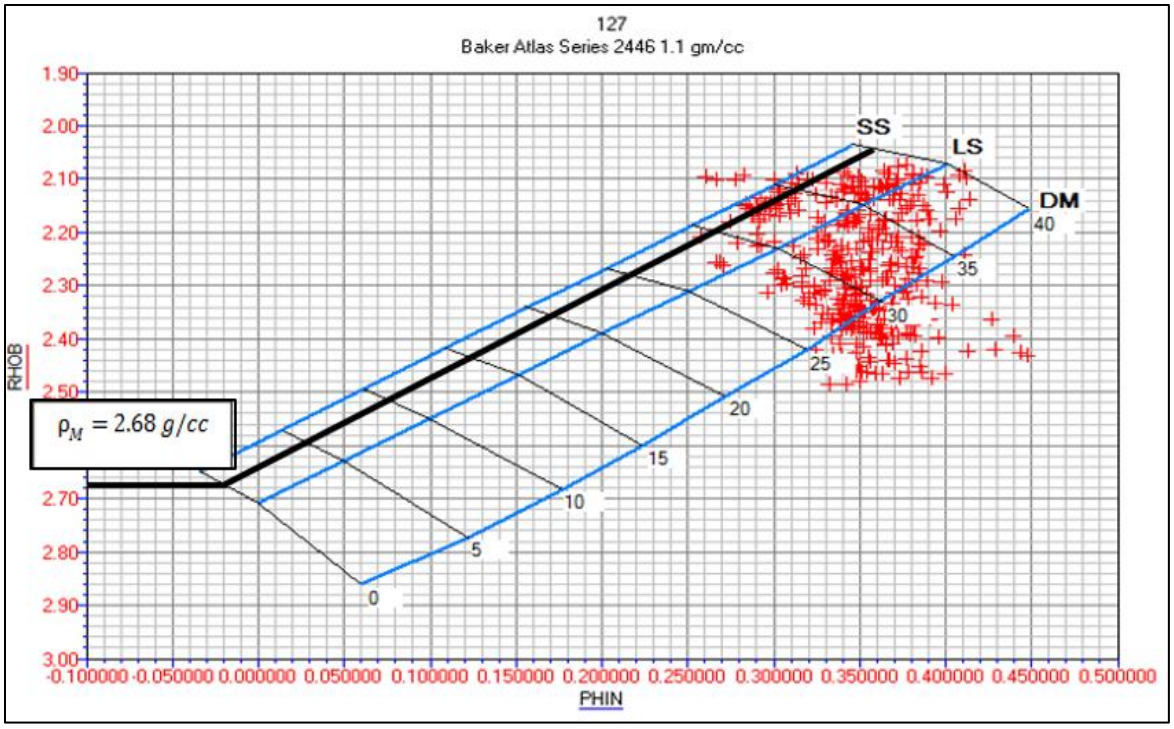

Figure 18: Lithology Determination with density of 2.68 g/cc for WB Layer

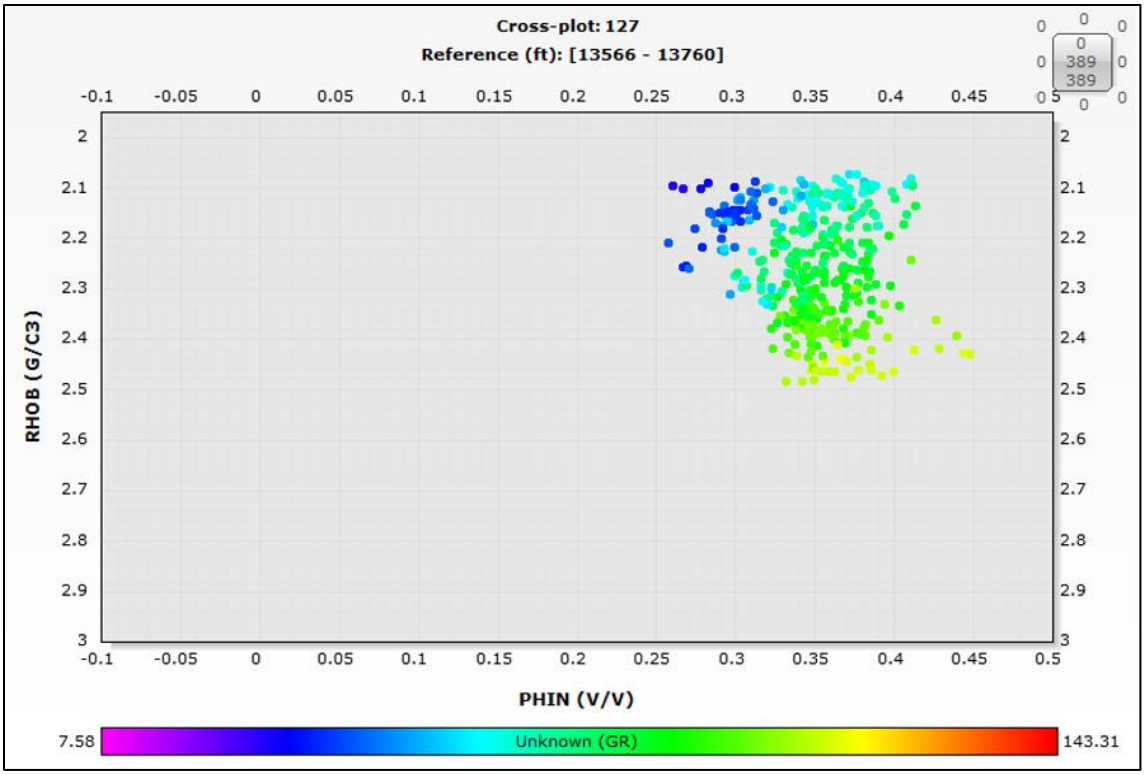

Figure 19: Demonstration of Shale Effect on Lithology for Well 127

3.4 Shale Volume

In determining shale volumes for each well, the first step is to find the sandstone and shale baselines for each well from the Gamma Ray log. These baselines were then averaged across the producing wells and used as the GR_clean and GR_shale parameters. For average GR_clean a value of 12 API was used and for GR_shale a value of 120 API was used. Shale volume was calculated using **Eq. 1** and then corrected using the Stieber model, **Eq. 2**. The Stieber model was used because the Wolfcamp is a sand-shale reservoir.

$$V_{sh} = \frac{GR - GR_{clean}}{GR_{shale} - GR_{clean}} \quad \textbf{Eq. 1}$$

$$V_{sh\_ST} = \frac{V_{sh}}{3 - 2(V_{sh})} \quad \textbf{Eq. 2}$$

3.5 Porosity

To calculate porosity, the neutron porosity and bulk density logs provided were used, as well as the calculated shale volume log. Based on the lithology determination, the density porosity in water-filled sandstone units using **Eq. 3** was determined.

$$\emptyset_{D,ss} = \frac{\rho_{bulk} - \rho_{ss}}{1 - \rho_{ss}} \quad \textbf{Eq. 3}$$

It was then necessary to correct this value for the presence of shale. From this, the value for total porosity was determined. These calculations may be observed in **Eqs. 4 to 8**.

$$\emptyset_D^{sh} = \emptyset_D - V_{sh_{ST}} * \emptyset_{D,sh} \quad \textbf{Eq. 4}$$

$$\emptyset_N^{sh} = \emptyset_N - V_{sh_{ST}} * \emptyset_{N,sh} \quad \textbf{Eq. 5}$$

$$\emptyset_s = \frac{(\emptyset_D^{sh} + \emptyset_N^{sh})}{2} \quad \textbf{Eq. 6}$$

$$\emptyset_{sh} = \frac{\rho_{sh} - \rho_{bulk}}{\rho_{sh} - 1} \quad \textbf{Eq. 7}$$

$$\emptyset_T = \emptyset_s + V_{sh_{ST}} * \emptyset_{sh} \quad \textbf{Eq. 8}$$

Fig. 20 shows the relationship for well 127 between the core porosity and the calculated porosity corrected for shale, which was used to confirm the calculation of total porosity. The equation of the best fit line is y = 0.090762 + 0.564285x with an r value equal to 0.785. The correlation is strong and the next step can be taken.

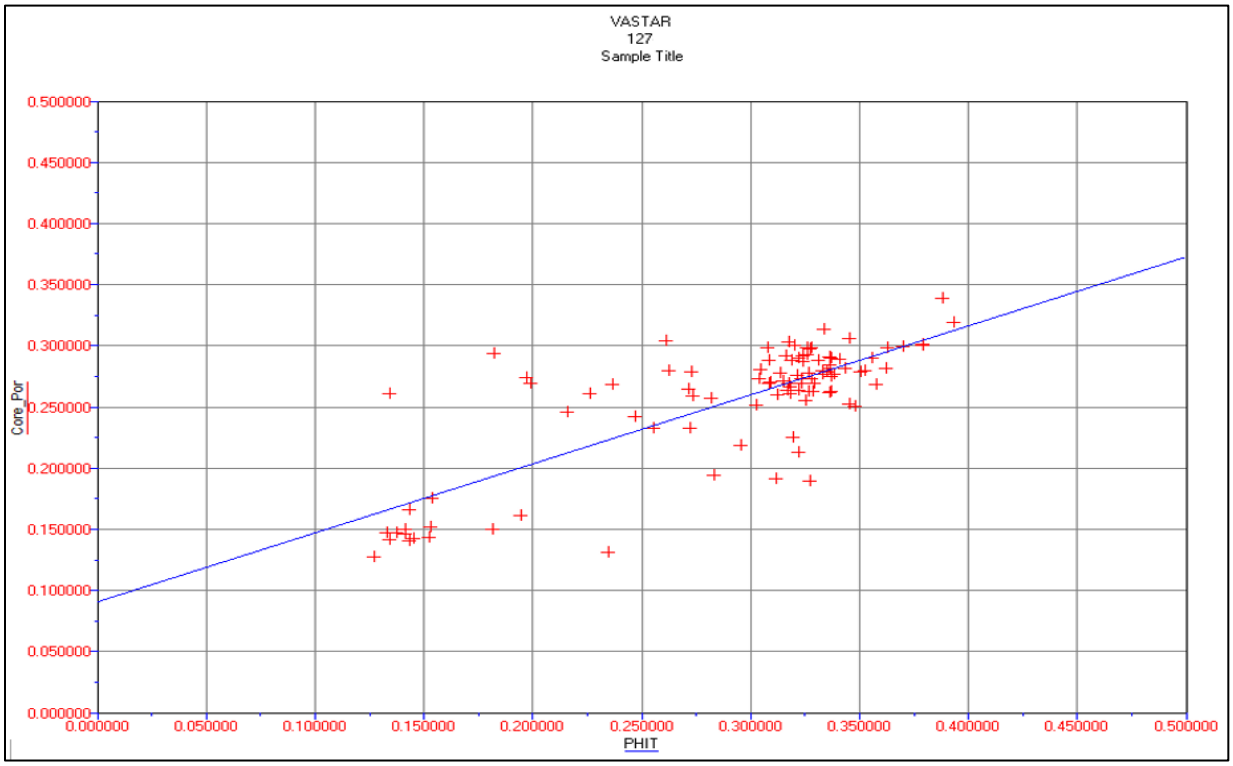

Figure 20: Relationship Between Core Porosity of Well 127

3.6 Water Saturation

To calculate water saturation, the Dual-Water Model was used due to the shale within the Wolfcamp formation (Malik et al., 2013). Provided core analysis data (Pioneer Natural Resources Co., 2016) was used to estimate cementation exponent (m) and saturation exponent (n). An average was calculated for both parameters for this well. Archie's equation (**Eq. 9**) was used along with **Fig. 21** to estimate the tortuosity factor (a).

$$F = \frac{a}{\emptyset^m} \quad \textbf{.....Eq. 9}$$

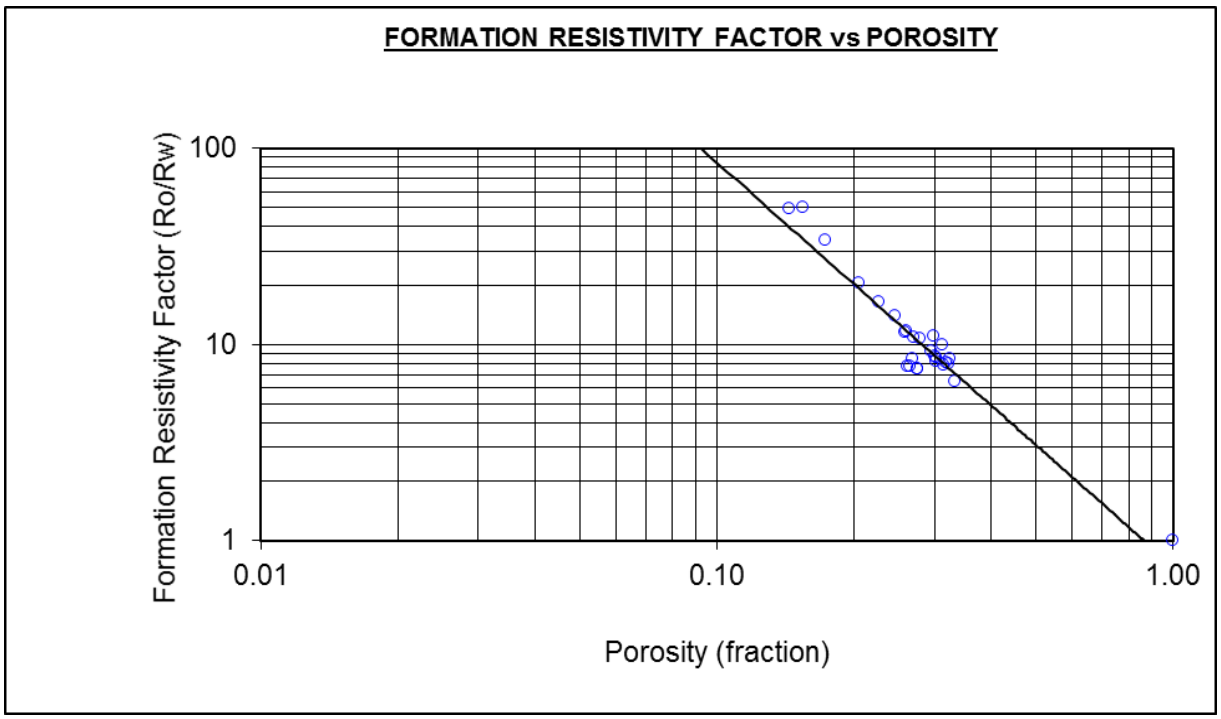

Figure 21: Formation Resistivity Factor vs Porosity Used for Tortuosity Determination

Using the slope of the line (m=1.82) and a point that lies on the fitted line, Archie's equation was solved for a. Comparison with other Formation Resistivity Factor vs. Porosity plots yielded similar results. The water resistivity was estimated using the water resistivity featured in the core data analyses. The water resistivity is equal to 0.076 ohm at 75° F, and by using **Eq. 10** the calculated water resistivity equal to 0.034 ohm-m.

$$R_2 = R_1 \frac{T_1+6.77}{T_2+6.77} \quad \textbf{Eq. 10}$$

This value was used for comparison purposes in the overall analysis. The first step in the dual water model is to determine the water resistivity and the clay bound water resistivity using

Pickett-Plots. It was also necessary to create a log track for clay bound water saturation because it is necessary for further calculations, which were calculated using **Eq. 11**.

$$\frac{1}{R_t} = \frac{\emptyset_t^m S_{wt}^n}{a} * \left(\frac{1}{R_w} + \frac{S_{wb}}{S_{wt}} * \left(\frac{1}{R_{wb}} - \frac{1}{R_w}\right)\right) \quad \textbf{Eq. 11}$$

To determine the water resistivity a permeable, fully water saturated zone in well 127 at a depth interval of 13,768' – 13744' was used. A Pickett-Plot was created using this interval and determined a water resistivity constant, which is displayed in **Fig. 22**. The same procedure was used to determine clay bound water resistivity constant using a shale zone interval at depths of 12,510' – 12,530', which is displayed in **Fig. 23**. Finally, the entire Wolfcamp shale reservoir can be examined. Using the constants previously mentioned, the overall water resistivity and clay bound water resistivity of the Wolfcamp shale interval was found to be 0.032 ohm-m and 0.013 ohm-m, respectively (**Fig. 24**). After determining these values, the dual water model can be implemented, **Eq. 12**, to calculate and create a log track for total water saturation.

$$S_{wb} = V_{sh\_ST} * \frac{\emptyset_{sh}}{\emptyset_t} \quad \textbf{Eq. 12}$$

Fig. 25 shows the relationship for well 127 between the core water saturation and the calculated total water saturation, which was used to confirm the method used. The equation of the best fit line is y = -0.048875 + 0.903595x with an r value equal to 0.849 (**Fig. 26**).

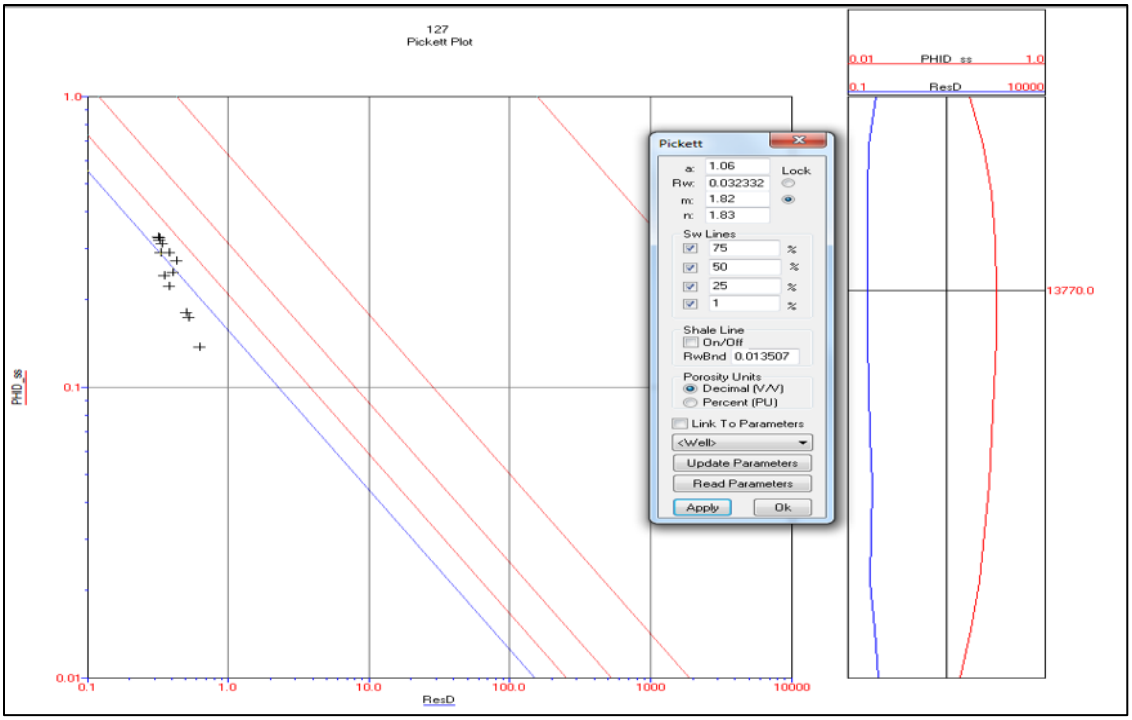

Figure 22: Determination of Permeable Fully Water Saturated Zone

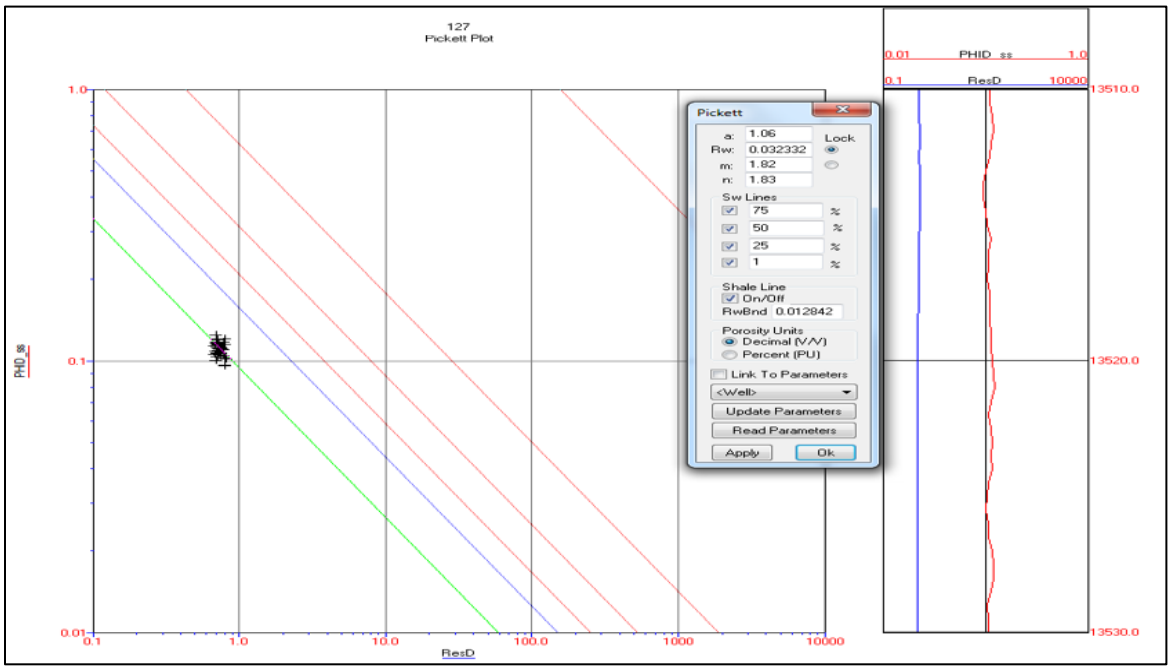

Figure 23: Determination of Clay Bound Water Resistivity

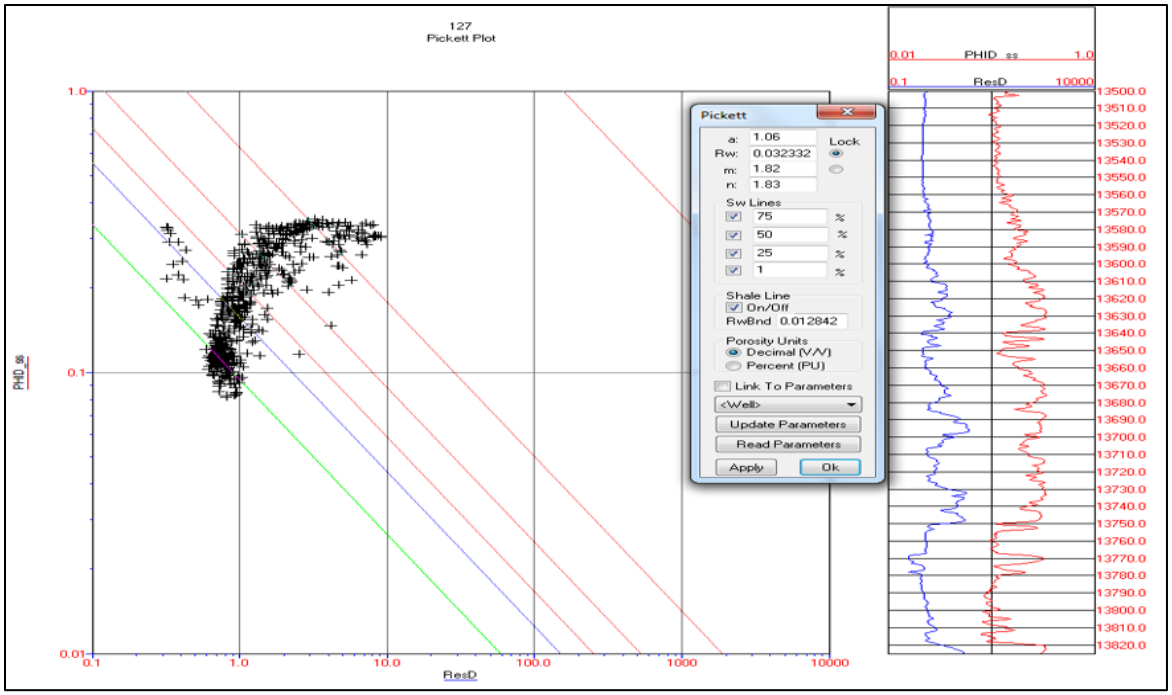

Figure 24: Determination of Water Resistivity and Clay Bound Water Resistivity

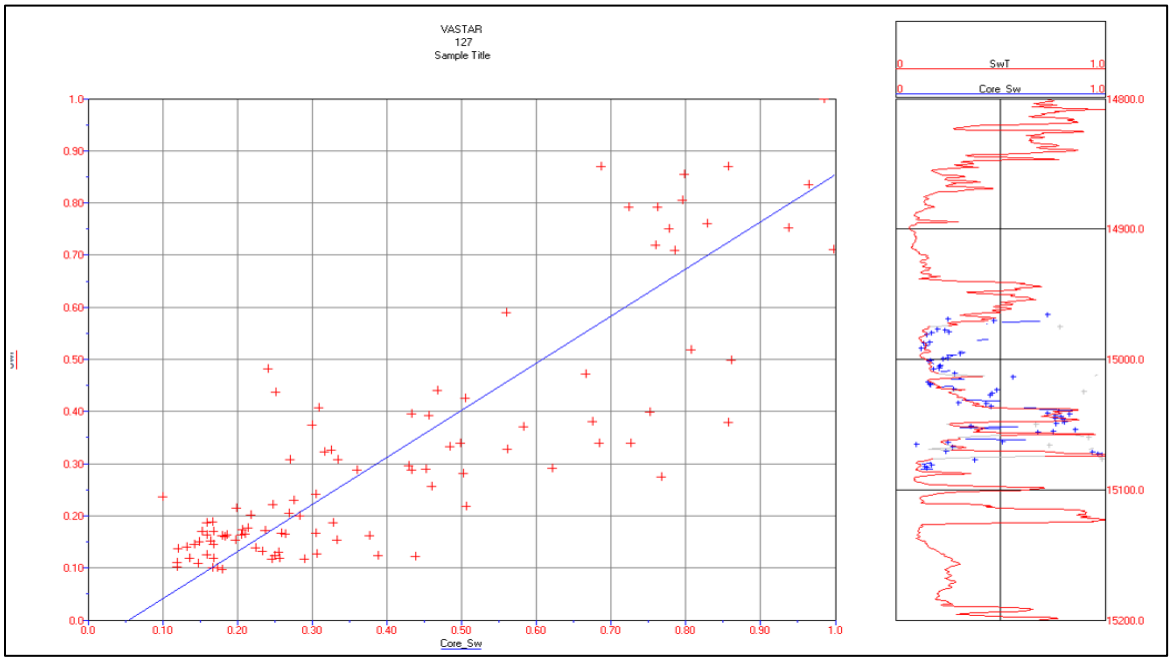

Figure 25: Crossplot of Calculated and Core Water Saturation

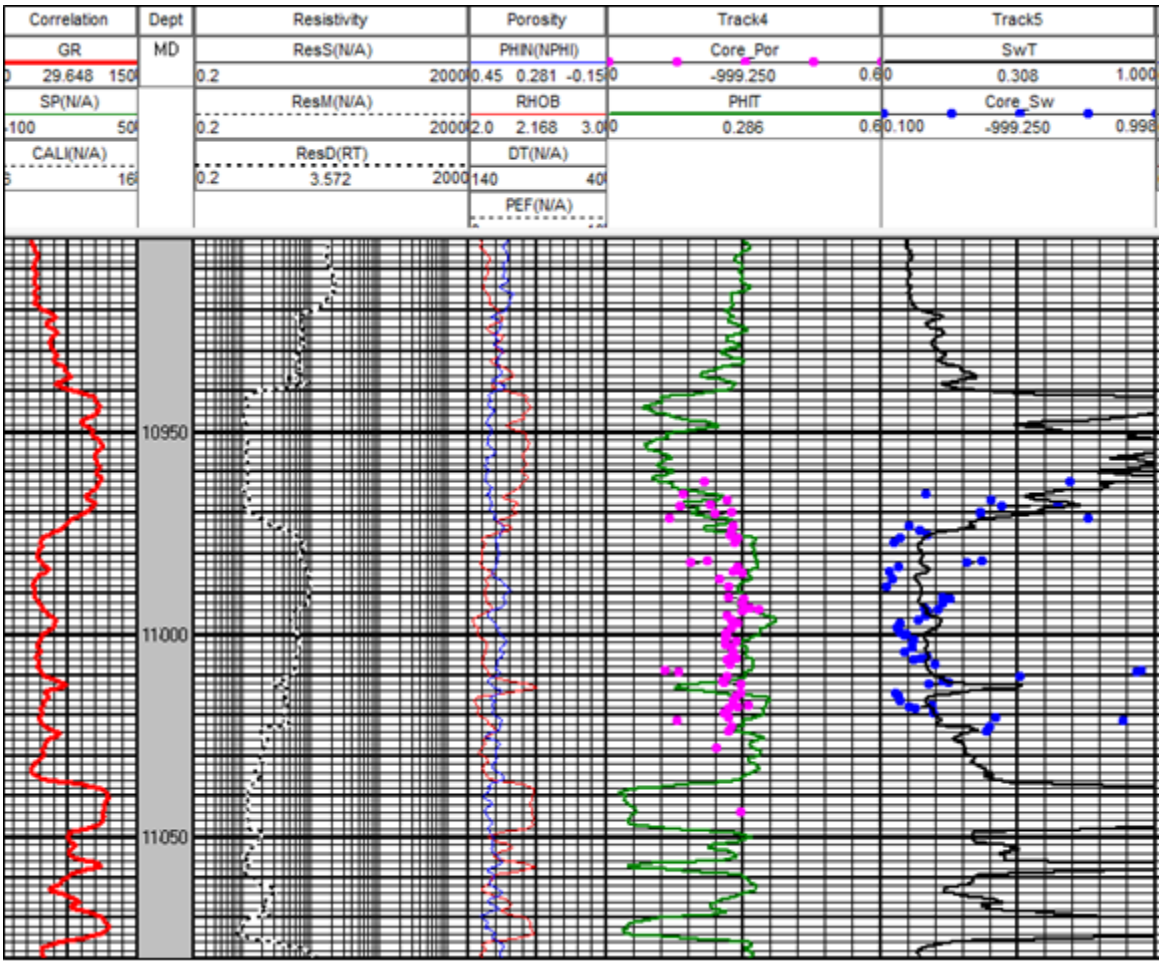

Figure 26: Log Tracks Displaying Calculated and Core Water Saturation

3.7 Permeability

Permeability was determined based on the correlation obtained from core permeability - porosity cross plots (Malik et al., 2013). This provided an equation that was imported into GeoGraphix and calculated permeability. **Figs. 27** and **28** are the crossplots that were used to determine the linear relationship between porosity and permeability. It was necessary to determine two different equations, because as the porosity values exceed approximately 27 percent, the relationship begins to change. The data points begin to form a cluster and there is not as large of an increase in permeability with a change in the higher porosity values. Both

equations were used in the calculations for the permeability log. **Fig. 29** shows the relationship for well 127 between the core permeability and the calculated permeability, which was used to confirm the method used. The equation of the best fit line is y = 91.548714 + 1.185353x with an r value equal to 0.652.

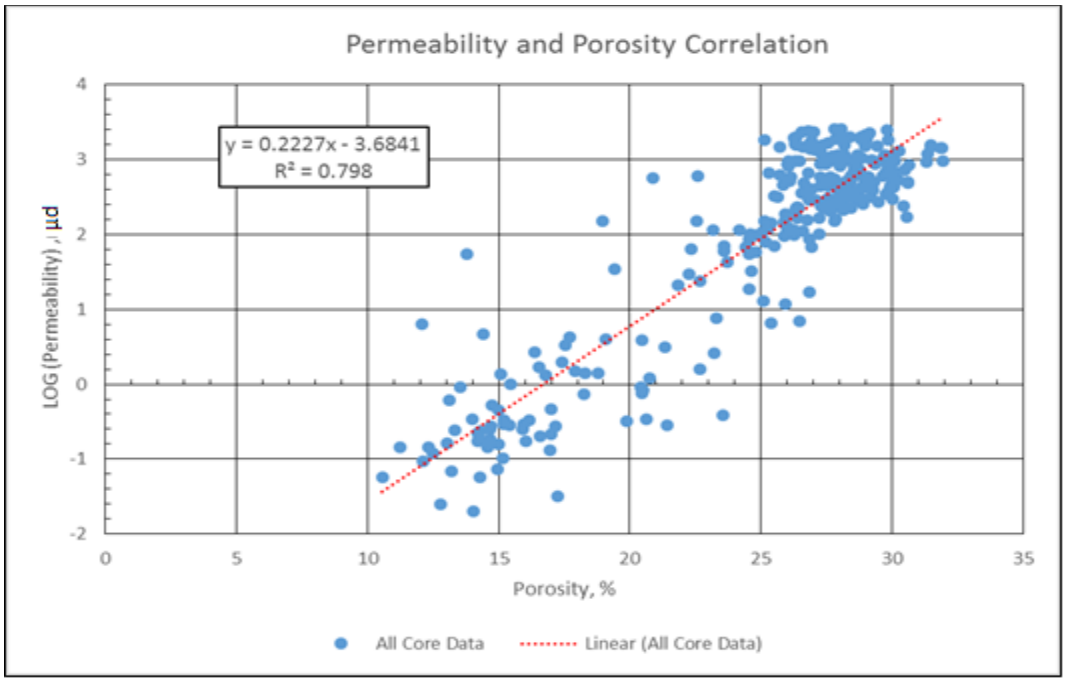

Figure 27: Correlation and Equation used for Porosity Less Than 27 Percent

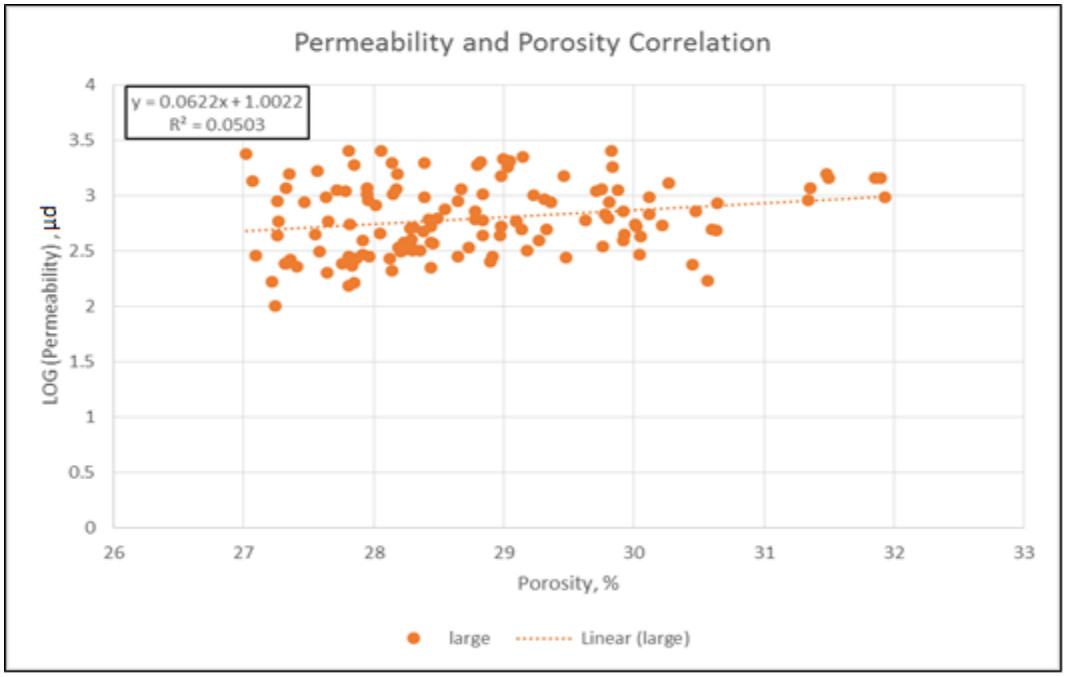

Figure 28: Correlation and Equation used for Porosity Greater Than 27 Percent

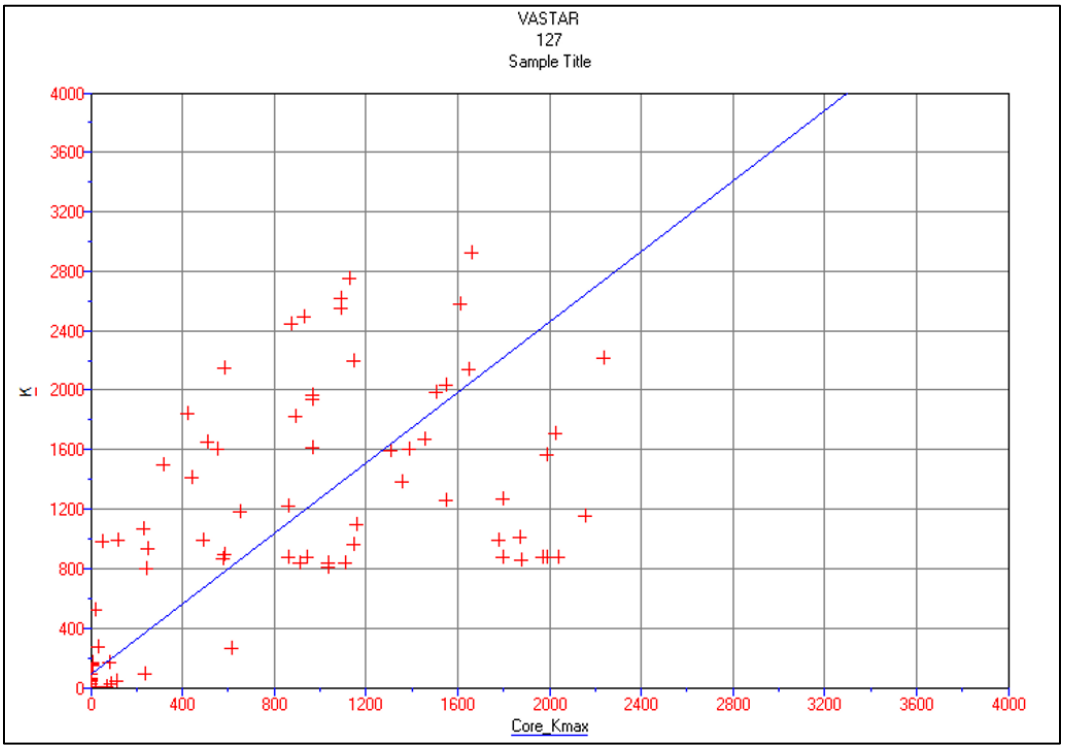

Figure 29: Correlation Between Core and Calculated Permeability

3.8 Net Sand Determination

Net sand was determined by implementing cutoffs for the shale volume and porosity (Malik et al., 2013). To determine the first cutoff, a semi-log plot of permeability versus porosity was created. Cutoffs are determined from crossplots by finding where the two highest concentrated sets of data are located, and dividing them vertically and horizontally. **Fig. 30** shows the determination of porosity cutoff to be 19 percent. The shale volume cut-off was determined following the same approach. A Cartesian graph was used to plot shale volume versus porosity to determine a shale volume cutoff of 45 percent, which is shown in **Fig. 31**. After determining these cutoffs, the requirements were defined as necessary to be considered net sand. These requirements include having shale volume less than 45 percent and a porosity value of at least 19 percent.

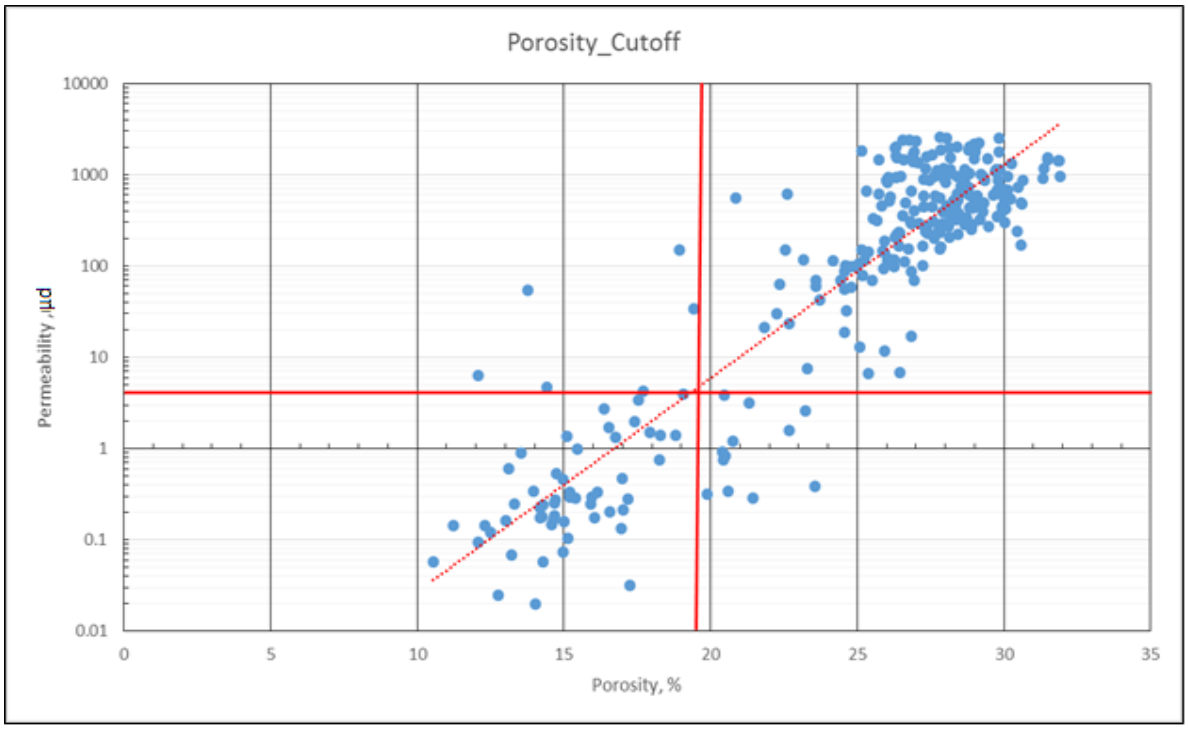

Figure 30: Determination of Porosity Cutoff Equal to 19 Percent

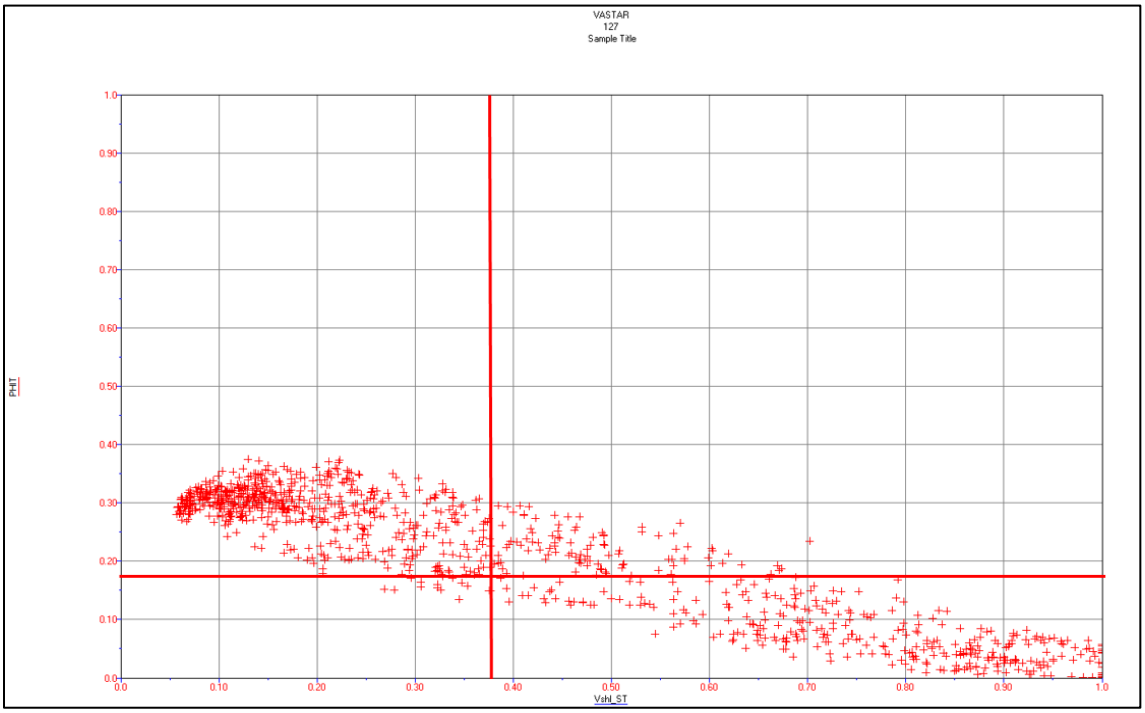

Figure 31: Determination of Shale Volume Cutoff equal to 45 Percent

3.9 Fluid Contacts

In order to determine the oil water contact (OWC) for the Wolfcamp, the resistivity logs (Pioneer Natural Resources Co., 2016) were primarily used (Malik et al., 2013). From the resistivity logs the lowest point of oil in the Wolfcamp formation is at approximately 13,270' (**Fig. 32**).

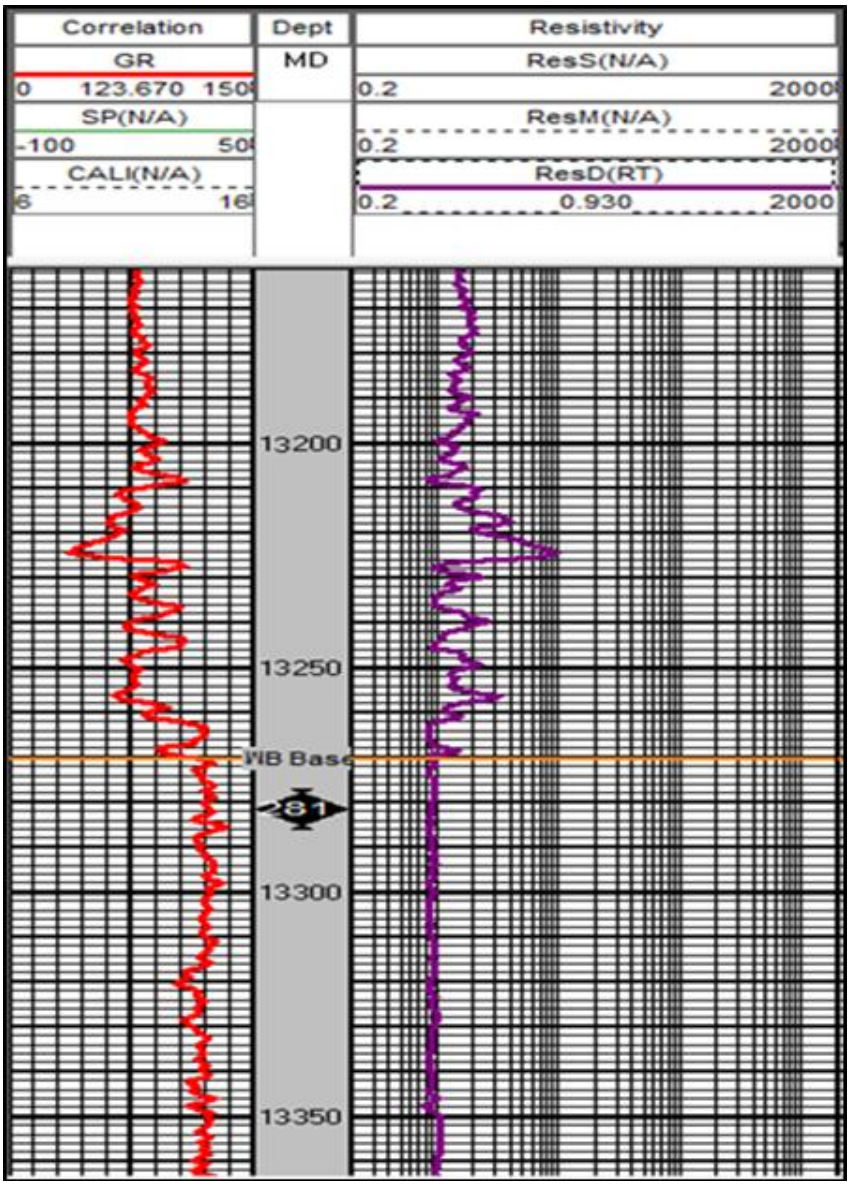

Figure 32: Lowest Point of Oil is Determined to be 13,270'

3.10 Petrophysical Properties of Interest

Fig. 33 shows the playbacks of type log well 127 (Pioneer Natural Resources Co., 2016). Average petrophysical properties including gross sand thickness, net sand thickness, net to gross ratio, shale volume, porosity, water saturation, and permeability were obtained using curve data statistics. The results are organized and tabulated by each shale layer in **Table 1**.

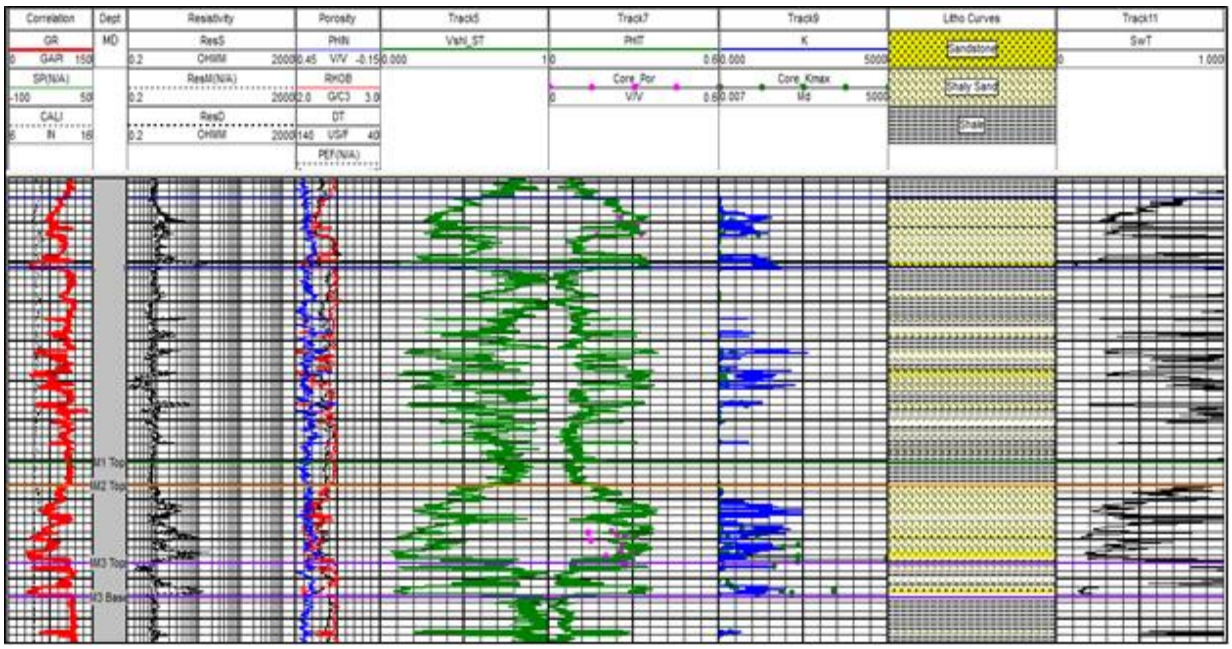

Figure 33: Playback of Well 127

Table 1: Petrophysical Properties of All 3 Layers

Wolfcamp-Well 127							
Zone	Gross Thickness, ft	Net Thickness, ft	N/G Ratio	Shale Volume	Porosity	Water Saturation	Permeability, µd
A	60.1	0.0	0.00	0.78	0.10	1.00	0.10
B	193.0	85.5	0.44	0.38	0.26	0.50	688.62
C	86.0	23.0	0.27	0.58	0.16	0.79	448.34

3.11 Quantitative Assessment of Uncertainty in Petrophysical Property Estimates

The @Risk built-in function in Excel was used to quantitatively analyze the petrophysical properties obtained from available log and core data (Walls and Morcote, 2015). Monte Carlo Simulation is used to model the variation in different parameters in order to quantify the uncertainty associated with each parameter. A summary of the variation of the petrophysical properties of all three Wolfcamp shale layers including the minimum, average, and maximum

values are presented below (**Table 2** to **Table 5**). The petrophysical properties represented in the below tables are correlative to the research conducted in "Quantifying Variability of Reservoir Properties From a Wolfcamp Formation Core" (Walls and Morcote, 2015).

Table 2: Petrophysical Properties of WA

WA	Min	Mean	Max
gross sand thickness, ft	0.2	84.4	295.8
net sand thickness, ft	0.0	7.5	102.5
N/G ratio	0.00	0.06	0.35
Vshl	0.38	0.60	0.89
porosity	0.09	0.17	0.23
water saturation	0.48	0.77	1.00
permeability, µd	0.10	98.42	613.25

Table 3: Petrophysical Properties of WB

WB	Min	Mean	Max
gross sand thickness, ft	61.7	201.1	406.8
net sand thickness, ft	0.0	72.8	189.0
N/G ratio	0.00	0.36	0.75
Vshl	0.25	0.44	0.82
porosity	0.08	0.21	0.30
water saturation	0.30	0.58	0.99
permeability, µd	0.04	557.53	1,450.21

Table 4: Petrophysical Properties of WC

WC	Min	Mean	Max
gross sand thickness, ft	4.3	54.1	120.1
net sand thickness, ft	0.0	20.4	45.5
N/G ratio	0.00	0.37	0.85
Vshl	0.16	0.44	0.68
porosity	0.11	0.20	0.29
water saturation	0.47	0.77	0.96
permeability, µd	11.91	596.06	1,599.33

Table 5: Petrophysical Properties of Total

Total	Min	Mean	Max
gross sand thickness, ft	0.2	113.2	406.8
net sand thickness, ft	0.0	33.5	189.0
N/G ratio	0.00	0.26	0.85
Vshl	0.16	0.50	0.89
porosity	0.08	0.19	0.30
water saturation	0.30	0.71	1.00
permeability, μd	0.04	417.34	1,599.33

The results of the Monte Carlo simulation for each individual petrophysical property are shown from **Fig. 34** to **40**. The scope is over every well in the entire interval, from Wolfcamp A layer top to layer C base.

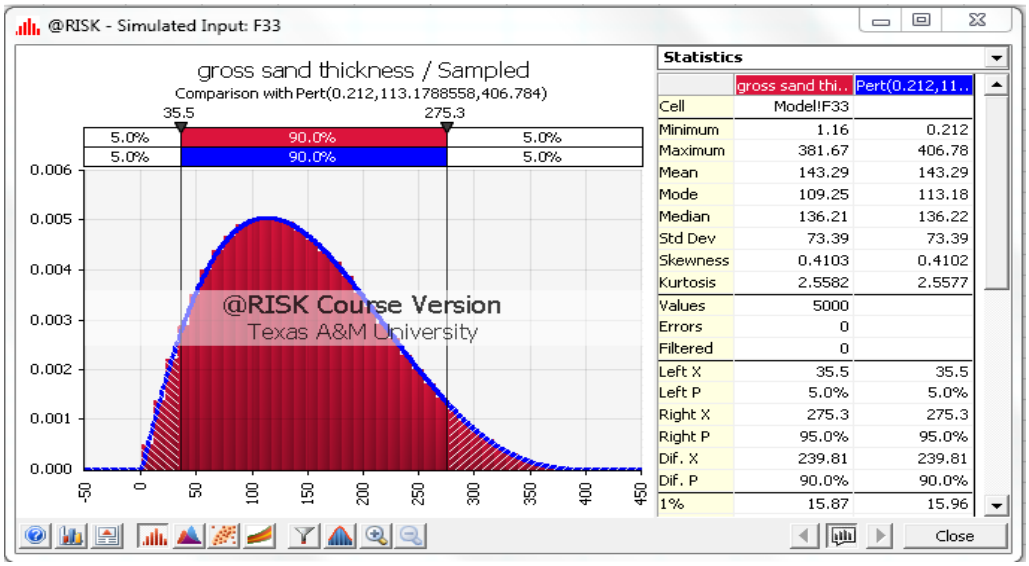

Figure 34: P5 and P95 Value of Gross Thickness

As shown in Figure 34, 5 percent of the gross thickness value of the shale zones falls below 35.5 ft, while 95 percent of the thickness falls below 275.3 ft. This provides an interpretation of variability or uncertainties of the petrophysical properties obtained.

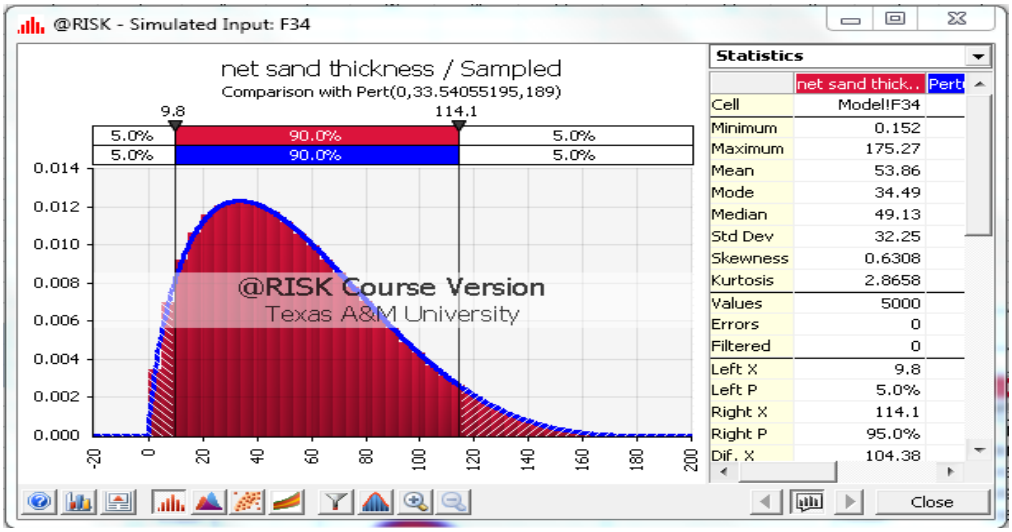

Figure 35: P5 and P95 Value of Net Thickness

As shown in Figure 35, 5 percent of the net thickness value of the shale zones falls below 9.8 ft, while 95 percent of the thickness falls below 114.1 ft.

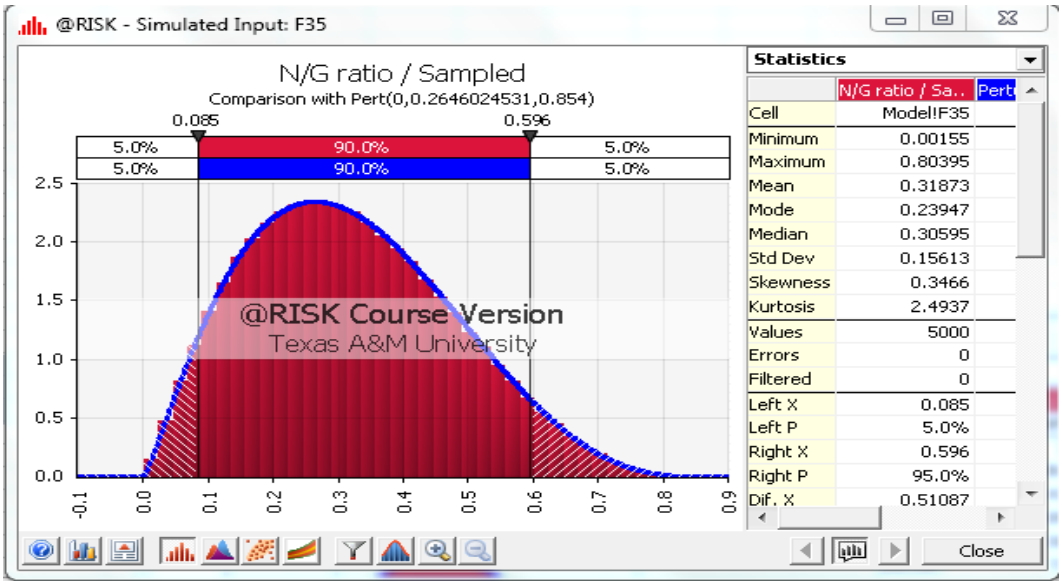

Figure 36: P5 and P95 Value of Net to Gross Ratio

As shown in Figure 36, 5 percent of the net to gross thickness ratio value of the shale zones falls below 0.085, while 95 percent of the thickness falls below 0.596.

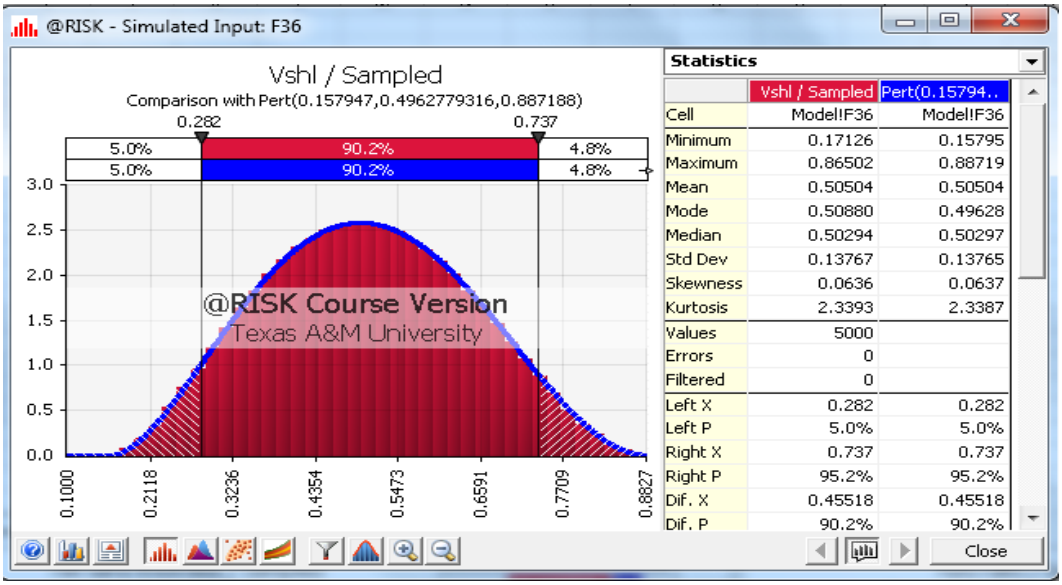

Figure 37: P5 and P95 Value of Shale Volume

As shown in Figure 37, 5 percent of the shale volume value of the shale zones falls below 0.282, while 95 percent of the shale volume falls below 0.737.

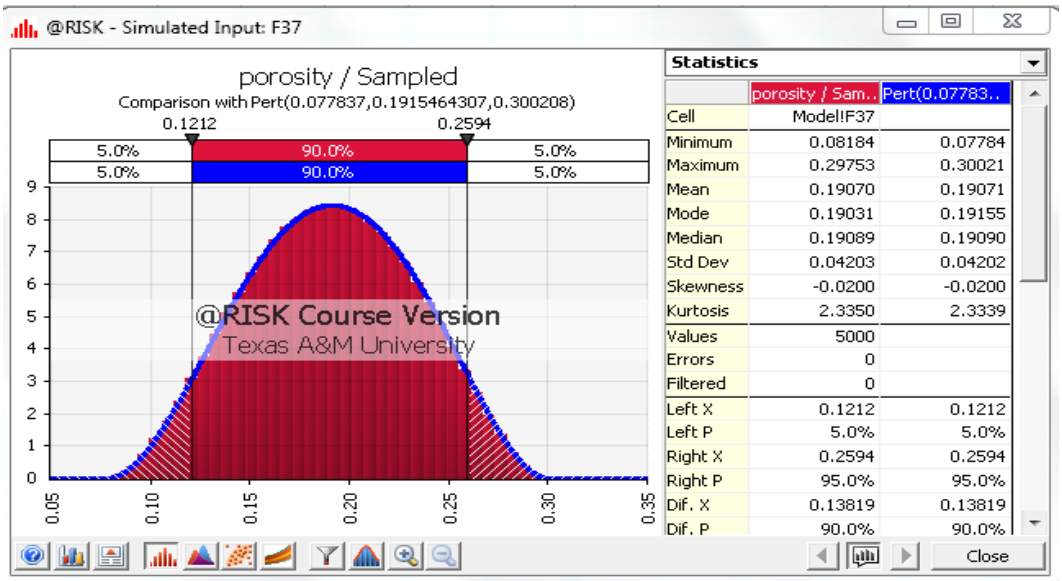

Figure 38: P5 and P95 Value of Porosity

As shown in Figure 38, 5 percent of the porosity value of the shale zones falls below 0.1212, while 95 percent of the porosity falls below 0.2594.

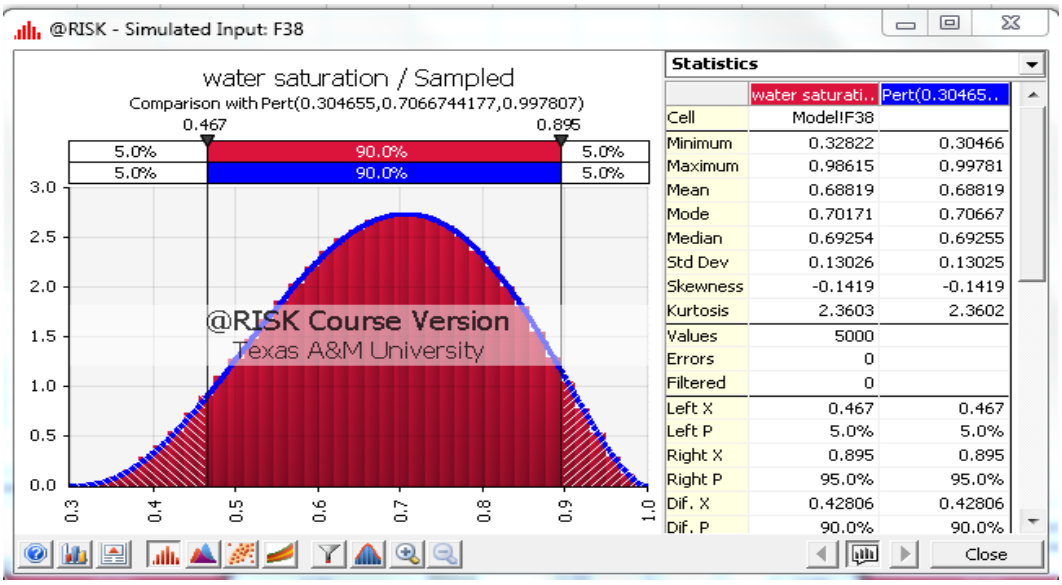

Figure 39: P5 and P95 Value of Water Saturation

As shown in Figure 39, 5 percent of the water saturation value of the shale zones falls below 0.467, while 95 percent of the water saturation falls below 0.0.895.

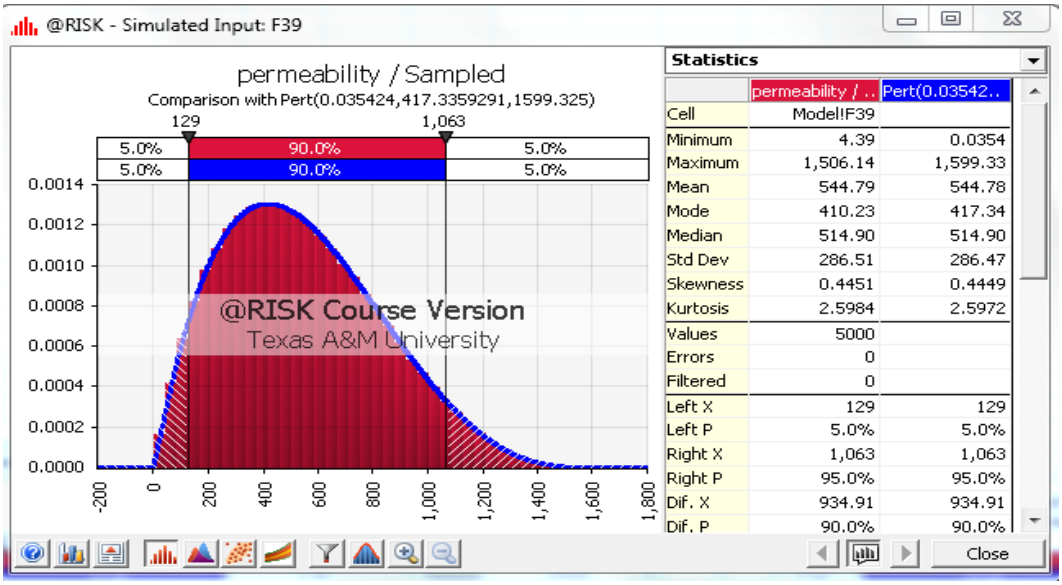

Figure 40: P5 and P95 Value of Permeability

As shown in Figure 40, 5 percent of the permeability value of the shale zones falls below 129 µd, while 95 percent of the permeability falls below 1063 µd

3.12 Conclusions of Petrophysical Analysis

The average, minimum and maximum gross thickness, net thickness, N/G ratio, Volume of shale, porosity, water saturation and permeability were determined for Wolfcamp A, Wolfcamp B and Wolfcamp C layers. These petrophysical properties were also determined for the Wolfcamp shales combined. The water oil contact was determined to be located at a depth of 13,300 ft in the Wolfcamp shales. The oil formation volume factor was also found to be 1.4 rb/STB.

4. RESERVOIR PERFORMANCE ANALYSIS

4.1 PLT Analysis

The production logging tool was run in well 127. The tool took measurements in the zones of interest to determine fluid entry points as well as the proportion of fluids entering the wellbore in these zones (Pioneer Natural Resources Co., 2016). Analysis was completed on the downhole flowing measurements for the well. Intervals in the report were given in measured depths, so the first step was to correlate these intervals to the different Wolfcamp shale zones (WA, WB, and WC) based off the tops and bases from previous logs. **Table 6** shows that for well 127, the majority of hydrocarbon production is coming from the WB zone and minimal water production from both WA and WC zones.

Table 6: Downhole Flowrates

Wolfcamp-Well 127			
Zone	Oil(bbl/d)	Gas(bbl/d)	Water(bbl/d)
A	51.25	38.45	48.71
B	362.19	58.22	13.08
C	7.81	0	1.95

4.2 PVT Analysis

PVT properties of a reservoir are very important when running reservoir simulations. Not only do they affect initial oil in place but also greatly impact the flow of the different fluids as a reservoir is being depleted. **Table 7** contains PVT data collected from a Wolfcamp sample with conditions of 184 °F and 3251 psia which is also the bubble point pressure. This data was from laboratory analysis of one sample although there were two samples from the Wolfcamp shale

available (Pioneer Natural Resources Co., 2013). Both samples presented very similar PVT results. This PVT data indicates a black oil reservoir due to a reservoir temperature lower than 250 ºF and an API gravity lower than 45 API. This conclusion corresponds with the production data as well. The production data suggests that this is a black oil reservoir due to the initial GOR being less than 1000 SCF/STB.

Table 7: PVT Data From Sample

Oil Compressibility	8.77 x 10-6	*1/psia*
Oil Viscosity	0.549	*cP*
Oil Gravity	33	*API*
Gas Density	0.756	*(Air=1)*
Formation Volume Factor	1.368	*RB/STB*
Bubble Point Pressure	3251	*psia*
Reservoir Temperature	184	*^{o}F*

4.3 Pressure Transient Test Analysis

The well test model was constructed using parameters from the given schematics and data (Pioneer Natural Resources Co., 2016). The payzone height for each well was found by using the thickness of the WB. The WB porosity was estimated to be 0.21 by averaging the porosity in WB for the well. After the model was constructed, the well was conditioned to the known reservoir parameters. The well was modeled as slanted a well in a homogenous reservoir. However, depending on the well, some wells could be modeled as single fault boundaries and some wells could be modeled as parallel fault boundaries. With the model set, the next step was to determine the correct permeability, skin, wellbore storage coefficient and fault distances through the use of the improve function. The primary goal of the model was to match the log-log plot, the semi-log plot and the history plot. **Fig. 41** is the buildup test for well 127.

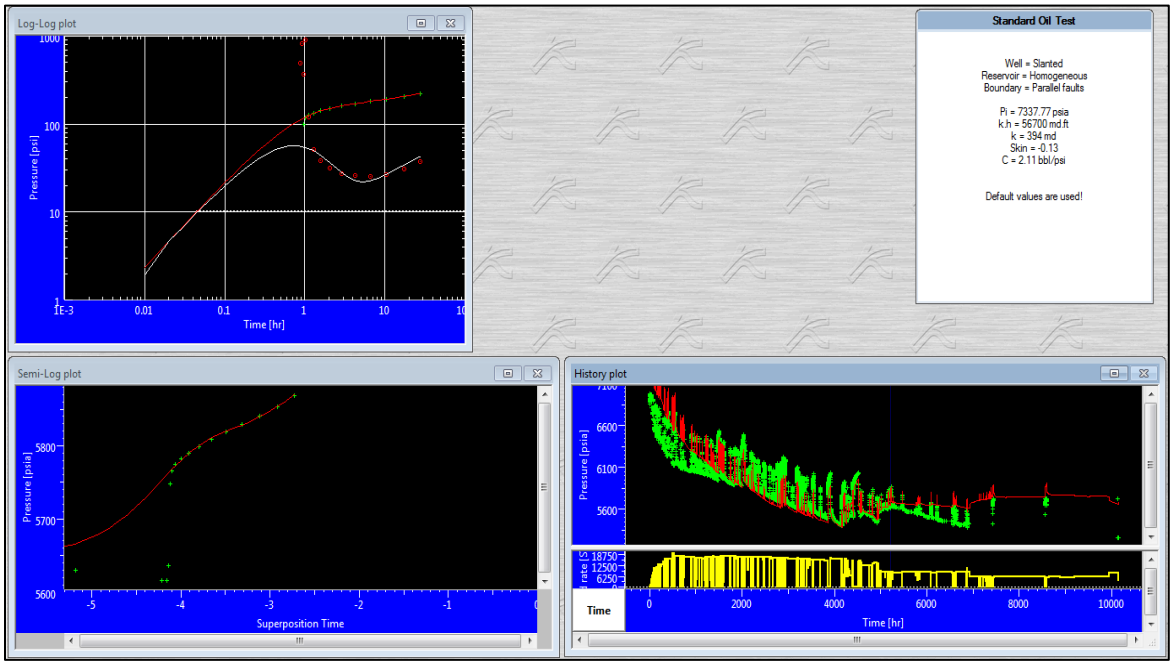

Figure 41: Well Test

The well test model for the buildup test of well 127 had a very close correlation. The log-log matched almost exactly, the semi-log plot matched almost as well as the log-log plot and the history plot matched well.

5. HISTORY MATCHING

5.1 Porosity and Permeability Map

The formulation of the porosity and permeability maps for the history matching portion of this study involved sGems. The methodology used involved kriging and cokriging (Zhao, Shan, et al., 2014). Within sGems a grid was created to import the well data and once loaded in as an object, the data was plotted on the Cartesian grid created. In **Fig. 42** below, the porosity of the wells is represented. From the variogram estimation a Max of 1200, Med of 270, Min of 90, azimuth of 50 and dip of 0 were determined. There was no nugget effect, only 1 structure, a sill of 1 and the curve type was exponential.

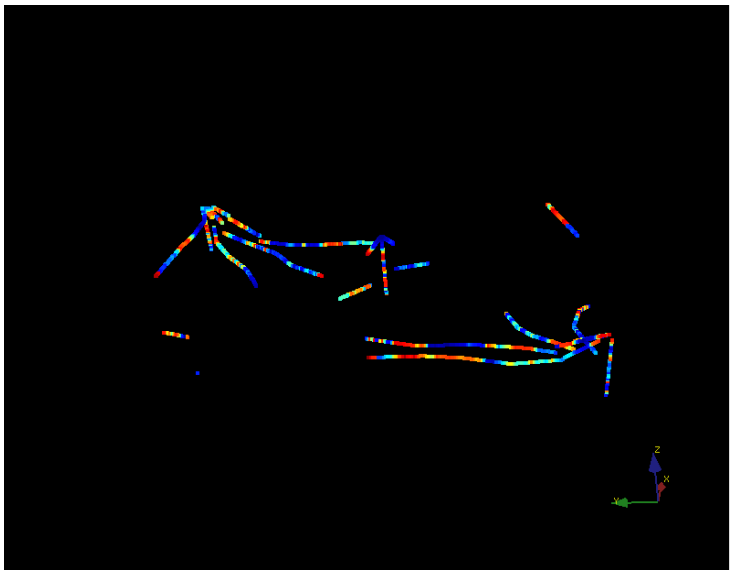

Figure 42: Initial Porosity Data

To generate the porosity field, a kriging simulation was performed to estimate the porosity throughout the grid. In the sGems program, the kriging function requires the hard data, a

search ellipsoid and the hard data variogram. Using the porosity as the hard data, an ellipsoid defined by Max/Med/Min equal to 4000, azimuth of 50, dip of 0, and the variogram that was previously created, the ordinary kriging function was used to generate a porosity field. The porosity field is represented in **Fig. 43** below for the kriging method.

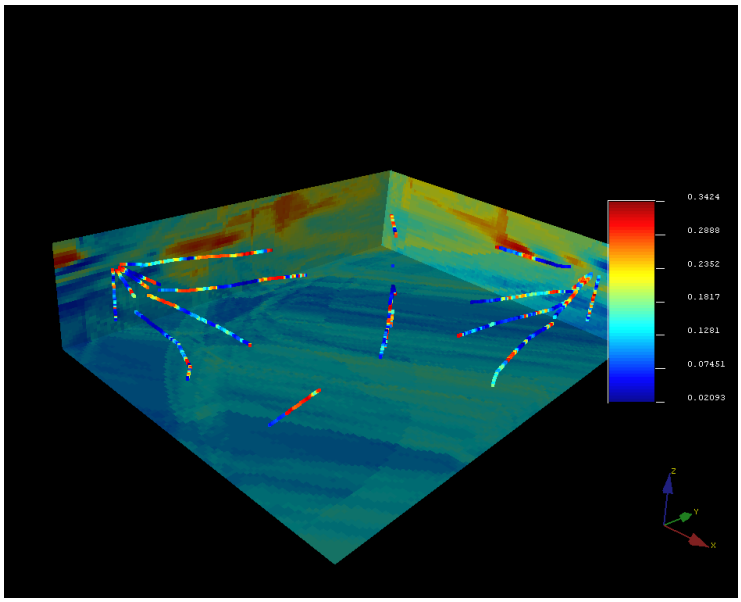

Figure 43: Porosity

The cokriging function in sGems allows for secondary data to refine the porosity field generated from the kriging function. Acoustic impedance data provided by Pioneer Natural Resources (2016) was used as the secondary data. The seismic data was loaded in on a new grid for cokriging. The seismic data is loaded in at the origin 0,100, 0 to coincide with the well coordinate and the new grid is negative in the z direction because the seismic data is loaded in from the top down. Now, to refine the porosity distribution using seismic data, the cokriging function is used. Mark Model 1 using simple kriging requires the SK mean of the primary and

secondary data, both data sets themselves, the ellipsoid for the primary data, the variogram for the primary data, the correlation coefficient of the primary to secondary data and the variance of the secondary data. The correlation coefficient between the primary and secondary data is determined from the plot of the small krig of porosity versus the impedance in **Fig. 44** below. This value was determined to be -0.178 as seen in Figure 44. With all of the requirements met, the cokrig simulation of porosity and measured impedance was run and generated the refined porosity distribution represented in **Fig. 45** below.

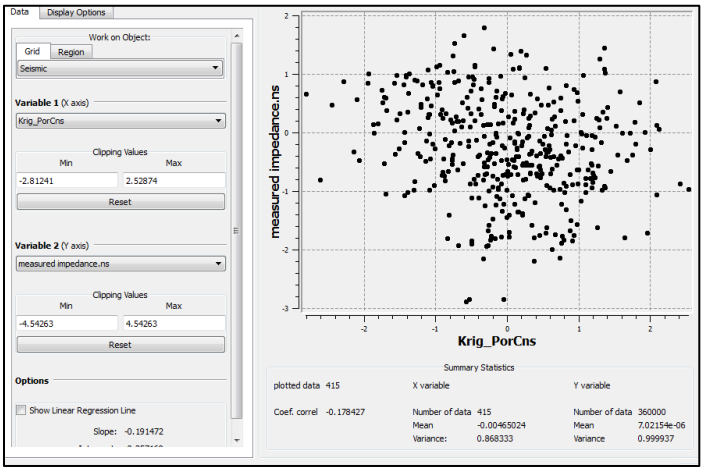

Figure 44: Coefficient Correlation Calculation

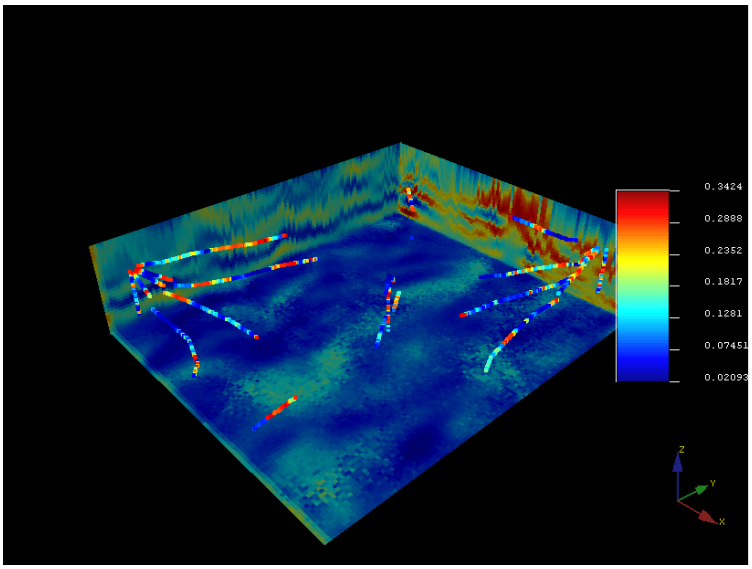

Figure 45: Cokrig Markov Model 1

When comparing the kriging and cokriging estimations, it is important to note the cokriging estimation is more refined due to the inclusion of the measured impedance data. Markov Model 1 was used because it functions the same in cases where the volume support of the primary and secondary data is similar, while requiring less inputs and having better computation time. Markov Model 1 Cokriged porosity in Figure 45 yields a better porosity field map than the kriging method because the ordinary kriging procedure used a purely estimated porosity that was found only through the porosity data. Conversely, the Markov Model uses a secondary set of data to refine the field map which is measured impedance in this case. The measured impedance correlates to the porosity throughout the field and allows to better estimate the porosity distribution throughout the field.

The porosity field map used for the case study is the Markov Model 1 Cokriged simulation and is the average of infinite Sequential Gaussian Simulations. The above process is

repeated to determine the permeability field map with the same constraints. Due to the nature of the data the permeability was found using Markov Model 1 Cokriged method as well and was measured against impedance as the secondary variable. The implementation of both porosity and permeability can be seen in the following section covering the CMG simulation where the porosity and permeability are gridded.

5.2 Generating CMG Simulation and History Matching

The information acquired throughout the project was then used to create a CMG simulation. The grid block is evenly spaced throughout the formation. In **Fig. 46**, the grid spacing for porosity is shown and in **Fig. 47** below, the grid spacing for permeability is shown.

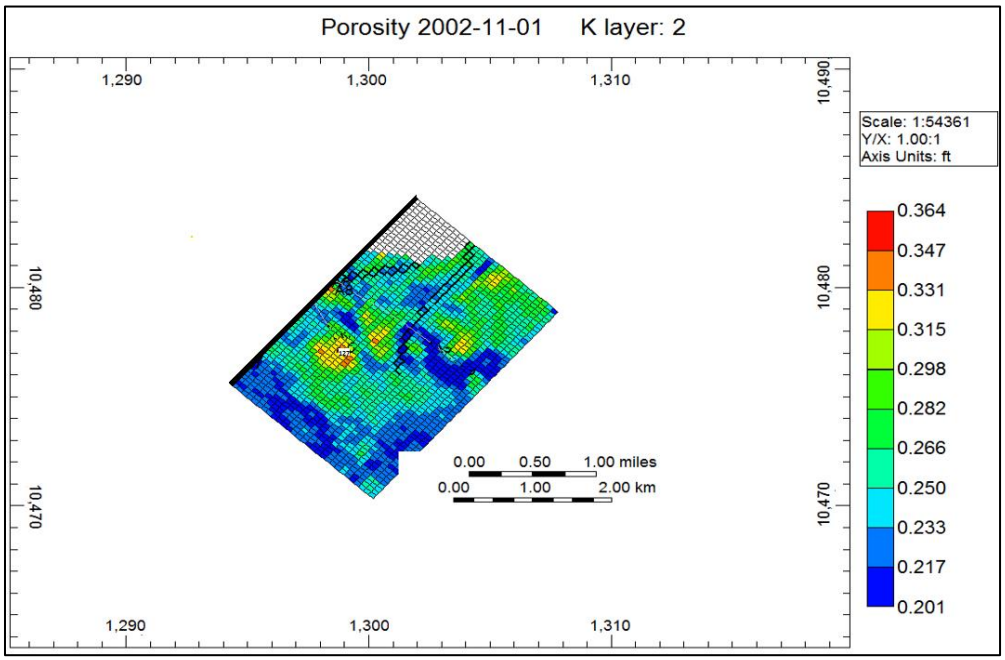

Figure 46: Porosity Map

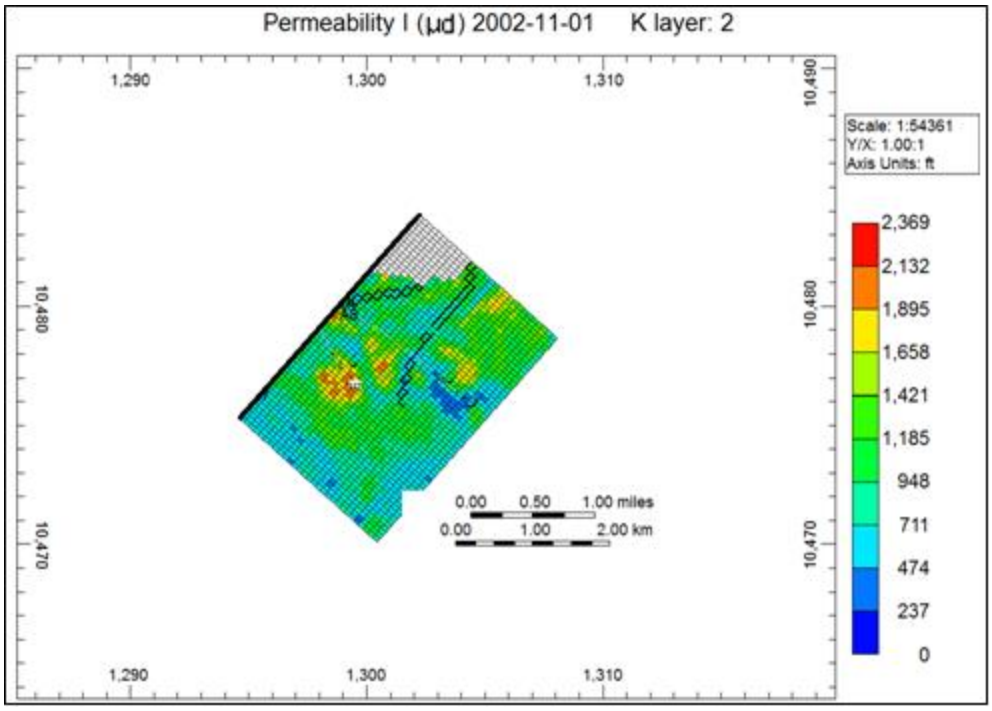

Figure 47: Permeability Map

The initial steps in CMG were to build the grid and define the reservoir characteristics found initially. From that point, the CMG simulation is initialized to get an understanding of where the formation characteristics need to be modified in order to better match the actual production rates for oil, gas and water. Porosity and permeability are the two major factors in effecting the history match but other characteristics were adjusted too, such as, saturation of oil and water and skin. Porosity and permeability were used to conduct the history match because Pioneer Natural Resources Co. (2016) data provided contained a quantity of reliable seismic data. The **Fig. 48** below is the final history match of well 127 after the formation characteristics have been adjusted through the CMG simulations (Pioneer Natural Resources Co., 2016).

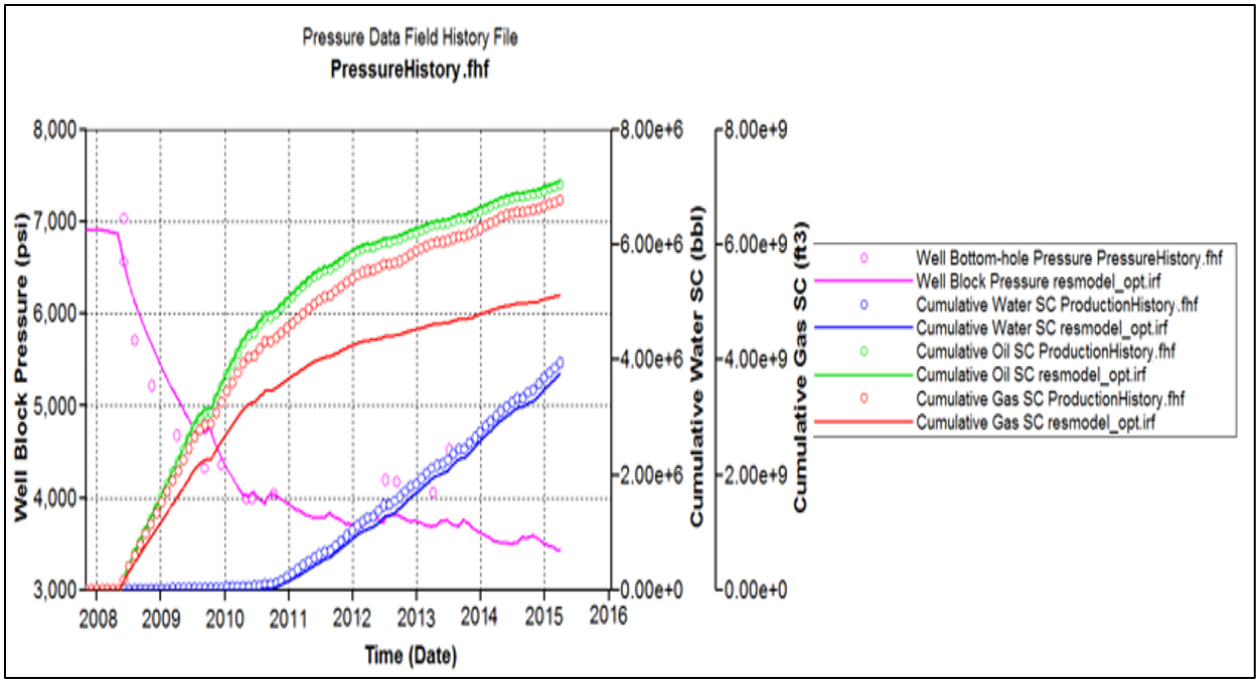

Figure 48: History Match

The history match plot is a chart of bottom-hole pressure (pink), cumulative water production (blue), cumulative oil production (green), and cumulative gas production (red). The circles for each plot represent historical data and the solid lines represent the reservoir model. The 3 curves bottom-hole pressure, water production, and oil production match almost perfectly whereas the gas production follows the same trend but isn't a perfect match. This was the closest the production and pressure history could get using the reservoir characteristics that were previously stated.

6. ANALOGOUS WELL

Using the data from the history match process, an analogous well was placed within the same reservoir. The original well was replaced with this new analogous well to maintain uniformity between the original and new well reservoir characteristics. The difference between the original history matched well and the new analogous well is the fracture conductivity tables of the SRV held at a fixed BHP. Fracture conductivity tables are considered an important geomechanical property because the permeability of the hydraulic fractures will change under different pressures, especially when propped open with different proppants. Hydraulic fractures are created when a section of the well is subject to great pressures that cause fractures to occur within the well which artificially increases the permeability. These artificial fractures are filled with sand that is commonly referred to as proppant. The closure of the fracture is affected both by the closure stress and the proppant material. Closure stress refers to the pressure seen by the fracture under specific pressure conditions and within the Wolfcamp shale the initial closure pressure is approximately 4,930 psi (Malik et al., 2013). The fractures within the shale layers will begin to lose permeability once the reservoir pressure of 4,930 psi is reached and the rate at which the permeability is decreased for each proppant was found from industry related data tables. To better understand the effect of the propped fracture conductivity tables on overall production, 9 different runs were created with different proppants.

Initially, the research consisted of finding fracture conductivity tables for the Wolfcamp and in doing the research, natural fracture conductivity results were found. However, the natural fracture conductivity tables cannot be used because the wells in the Wolfcamp are hydraulically

fractured (Zanganeh et al., 2015). Continuing from there, a single propped fracture permeability modifying table was found and the theory would be to vary this original fracture conductivity (Pei et al., 2013). This thought process was forgone because data tables for fracture conductivity for individual proppants were found. Three different types of proppants in two different sizes were use. These proppants and their fracture conductivities include ceramics (World Oil, 2015), resin coated (Badger Mining Corporation, 2016) and northern white sands (Badger Mining Corporation, 2016). Additionally, a ninth white sand of size 40/70 and its respective fracture table were used (US Silica, 2014).

The **Fig. 49** below shows the 9 different plots of propped fracture permeability with respect to the closure stress seen by the fracture and **Fig. 50** is a similar plot but with propped fracture conductivity in md-ft instead of permeability. The propped fracture conductivity tables are representative of multiple different types of sand to create a reliable comparison between differing fracture conductivity. The different sands used for these tables were size 30/50 and 40/70. The 30/50 and 40/70 sand sizes represented below are either ceramic, northern white sand, curable resin coated or precured resin coated sand. Both the size and type of sand used greatly affect the fracture conductivity. The ceramic sands have a higher crush resistance than the standard, cured and precured sands and such have the highest fracture conductivity. This is because as the fracture begins to close, the ceramic proppants are better at withstanding the closure stress than the other sands. When observing Figure 61, it is apparent that the order from most resistant to crushing to least resistant to crushing is ceramic, precured resin coated, curable resin coated and northern white sand. The Figure 61 also seems to have a clustering of the conductivity trends which reveals that the larger 30/50 sand also has a greater fracture

conductivity than the smaller 40/70 sands. Intuitively, the sand size implies that the 30/50 sand should have a greater increase in production than the 40/70.

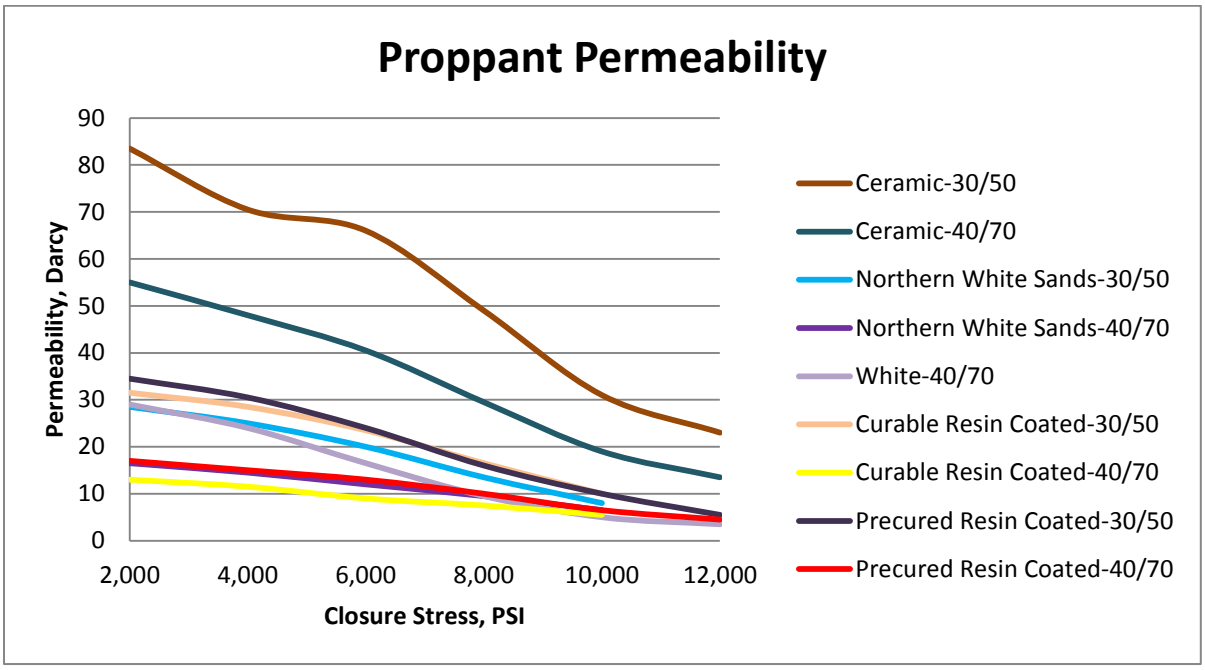

Figure 49: All 9 Proppant permeability Trends

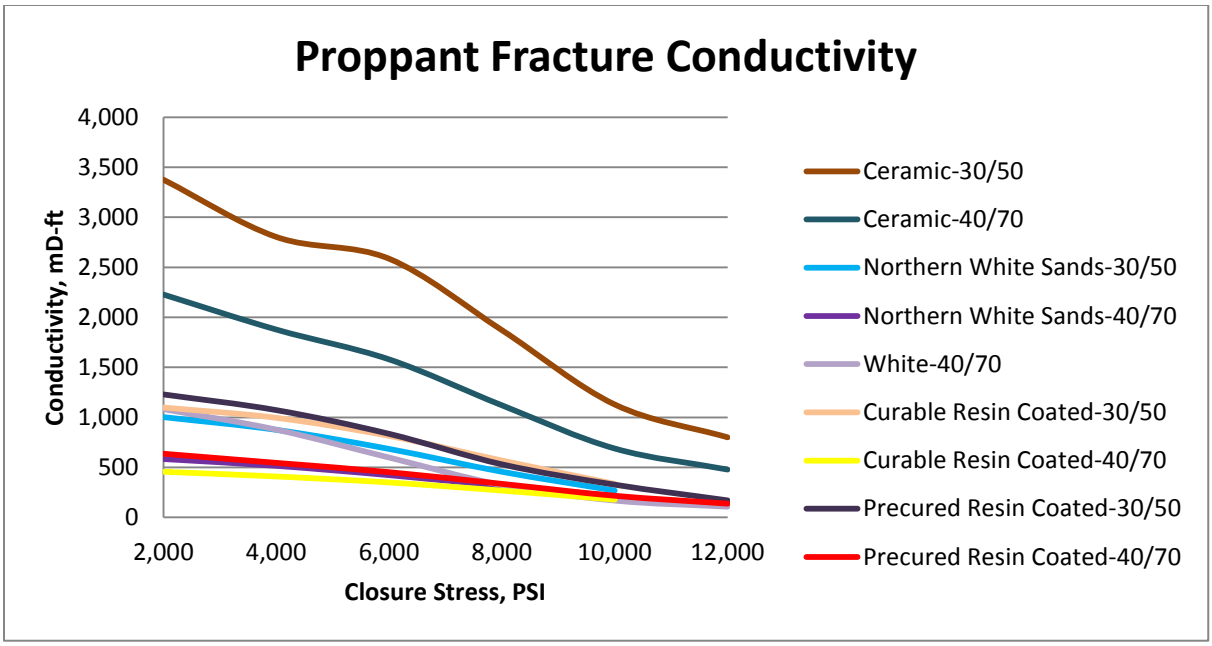

Figure 50: All 9 Proppant Fracture Conductivity

As mentioned previously, the fracture conductivity affects overall production by representing the decrease in permeability of the hydraulic fracture as a function of closure stress, otherwise known as fracture closure. This is called fracture closure because the high pressures in the hydraulic fracturing process creates fractures in the shale and as the reservoir pressure begins to decrease, the stress on the fractures increases. This fracture closure stress increases because the pressure holding these fractures open begins to decrease and causes the fractures to close. Standard permeability within the shale is not as greatly affected by the reservoir pressure, which is why the fracture permeability is much more drastic in change. This means that the fracture permeability of the shale is varied with respect to the closure stress which is dependent on reservoir pressure. Starting with the ceramic-30/50 case, at reservoir pressure of approximately 5,500 psi, the fracture conductivity table will come into effect when the pressure has been reduced to 4,930 psi. Additionally, as the reservoir begins to produce and the closure stress

begins increasing, you can see a clear and distinct decrease in the permeability of the hydraulic fractures. When the ceramic-30/50 scenario reaches a closure stress of approximately 10,000 psi, the permeability of the fracture is approximately 30 Darcy, meaning that the fracture permeability has been effectively reduced from 83.5 Darcy when at 2,000 psi. Following this same trend, it is easy to see how the permeability of the hydraulic fractures is affected by closure stress.

With this research heavily focused on hydraulic fractures and the proppant dependent fracture conductivity, it is important to correctly model the hydraulic fractures. An industry standard tool used to model the hydraulic fractures is Version10.9.35.0 of FRACPRO (2017) provided by CARBO Ceramics. This tool is used because of the precision in which proppants can be modeled within the lateral well design of the Wolfcamp wells and the ability to model the individual fractures in the intensive well design. The average horizontal well length in the Wolfcamp formation is approximately 10,000' and since the research focuses on the economic viability of the Wolfcamp, the average length was used in the well design. The optimal stage spacing for a 10,000 foot lateral is 240' with an average of 40 stages and each of these stages contains 5 clusters (Pioneer Natural Resources Co., 2018). If a stage spacing of 250' was used then 40 stages would fit perfectly but the wells are never drilled and completed under perfect conditions. In order to account for this, the 240' becomes the ideal spacing to allow for variance and non-uniformity within the horizontal itself. The **Fig. 51** below represents the horizontal well with transverse fractures in the Wolfcamp created with assistance from Lyle Lehman with Frac Diagnostics LLC.

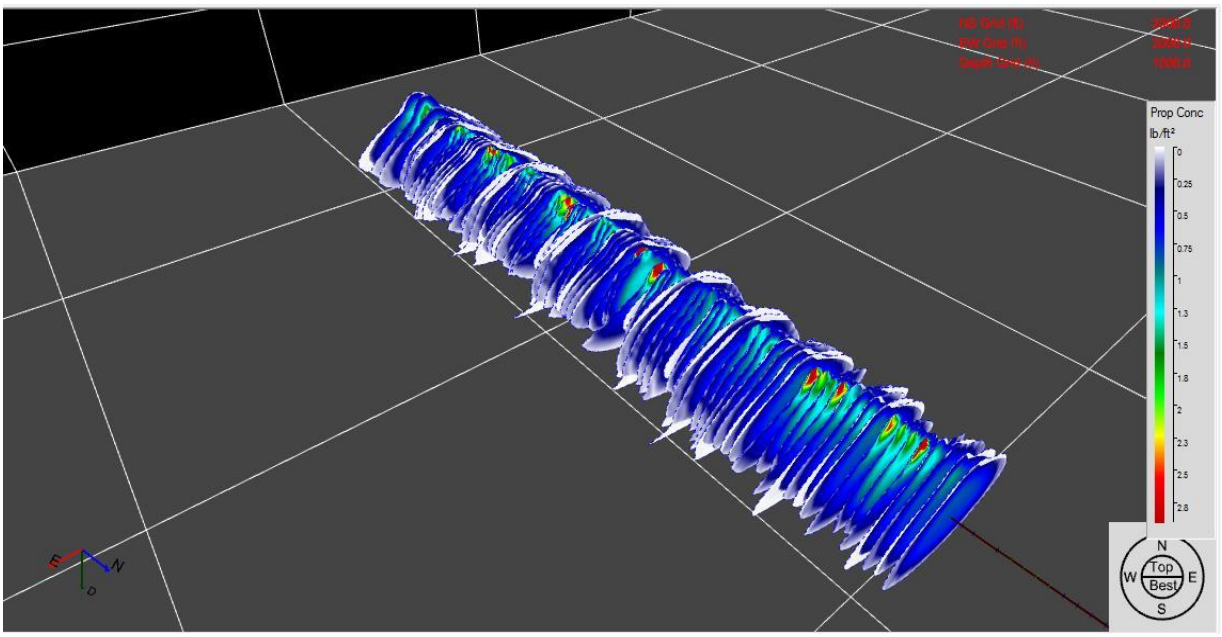

Figure 51: Horizontal Well

The well design itself is simple. The length of the horizontal, number of stages, stages pacing and clusters per stage are set and the petrophysical properties of the Wolfcamp are input. The simulation is run and clearly shows the propagation of the proppant into the fractures themselves. The fractures permeate outward from the well and the lb/ft^2 of proppant decreases greatly as it also permeates the well. This makes sense because the fractures are larger near the wellbore meaning more proppant by weight per area are present. The fracture size decreases as the distance from the wellbore increases and reduces the amount of proppant by weight per foot needed. The importance of the properly represented proppant distribution results from the reliance on the proppant dependent fracture conductivity tables. The accuracy of the fracture conductivity tables is dependent on the accuracy of the modeled fractures. In **Fig. 52** below, a single fracture cluster is shown as a side view so a better understanding of the modeled fractures may be observed.

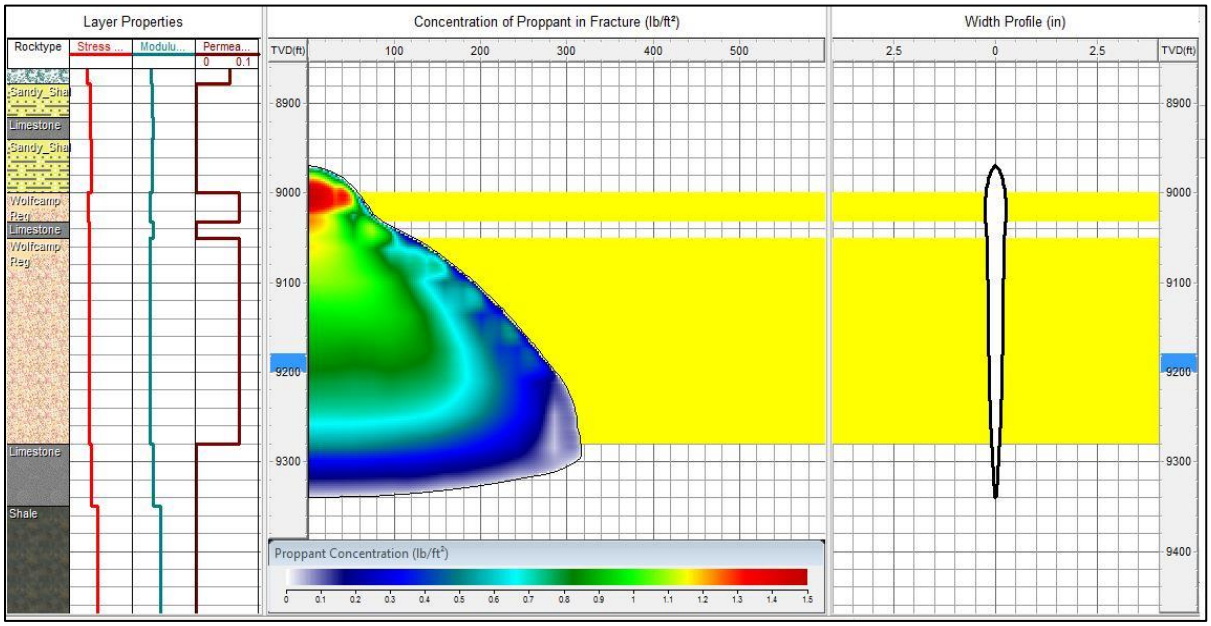

Figure 52: Fracture Design

Represented on the far left of Figure 52 is the formation rock type and the marbled pink coloring represents the Wolfcamp formation that the research focuses on. Following that rock type to the right, in red, is the formation stress that was previously discussed and is an important part of the fracture conductivity tables which are plotted against the closure stress. Similarly, in brown, is the permeability created from the fracture design which is determined from the propped fracture permeability referenced in Figure 49. The far right of Figure 52 is a representation of the fracture width profile in inches and the center of the image is the concentration of proppant within the fracture in lb/ft^2. As mentioned previously, the concentration of the proppant is greatest near the wellbore because that is where the fracture is the largest as seen in the width profile. The further into the formation the fracture permeates, the smaller the fracture width becomes and, in turn, reduces the concentration of the proppant. Near

the wellbore the concentration of proppant in the fracture is about 1.5 lb/ft^2 and at the extent of the fracture the concentration of the proppant is about 0.1 lb/ft^2. The fracture conductivity tables used for the different proppants work in conjunction with the propped fractures modeled and are considered one of the most important aspects of the simulation.

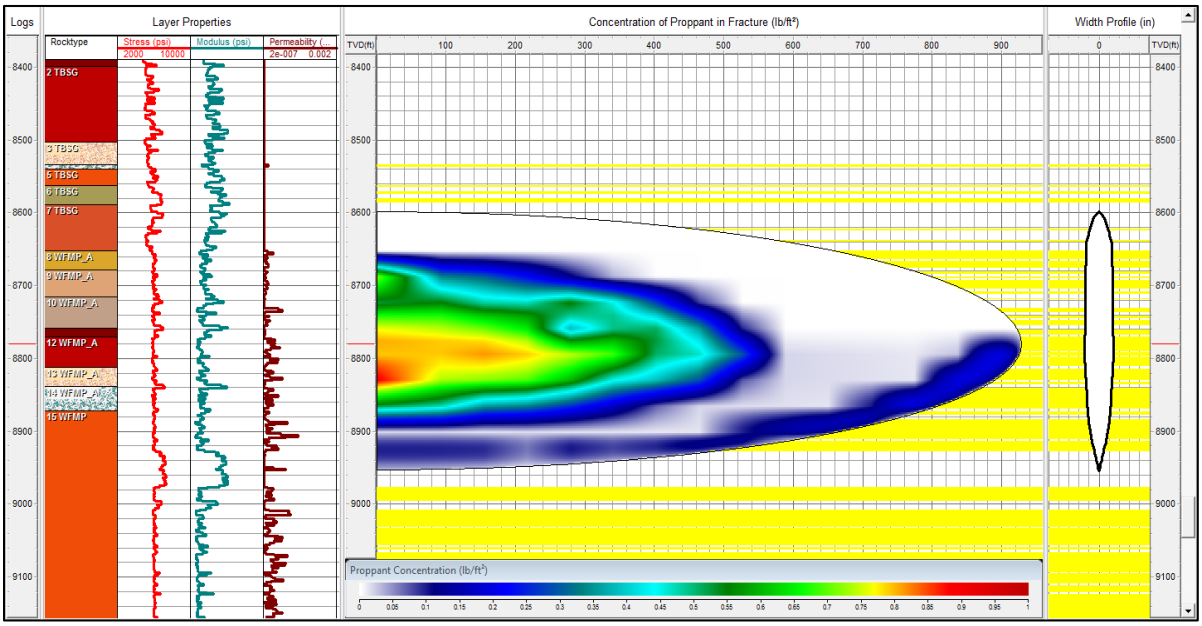

Figure 53: 40/70 Sand Propped Fracture

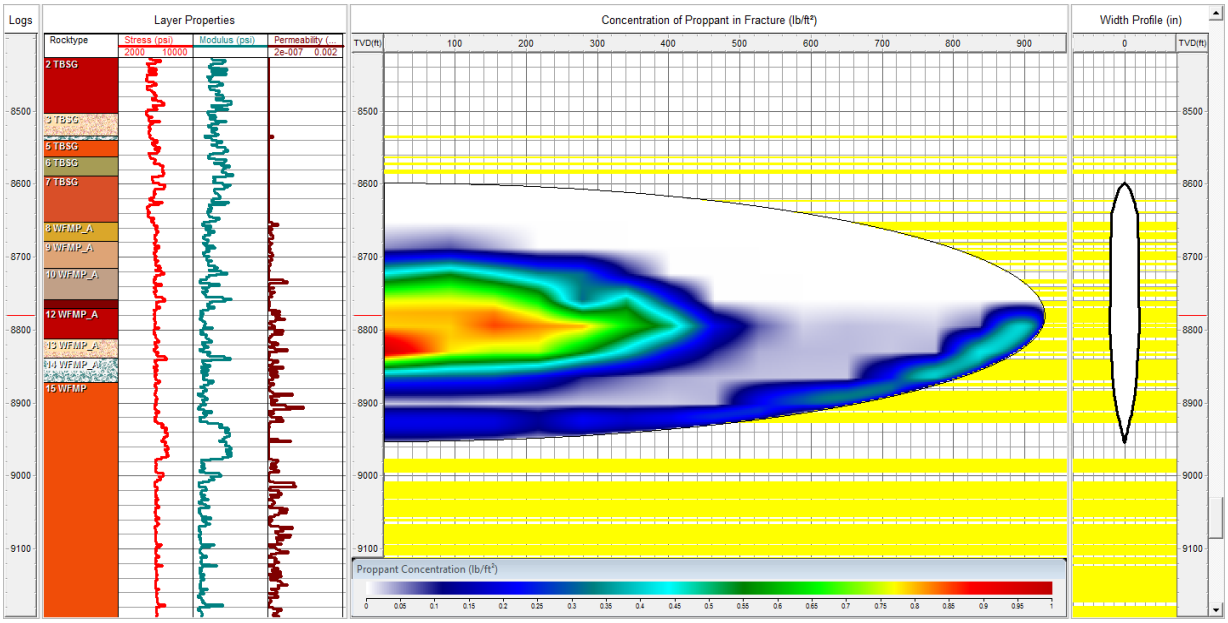

Figure 54: 30/50 Sand Propped Fracture

The fractures were created with the data acquired from Pioneer Natural Resources (2016) and NUTECH (2018). The **Fig. 53** above is a representation of a single cluster within one stage of the reservoir and the fracture is propped with size 40/70 sand. Size 40/70 sand is the smallest of the sands used and therefor propagates further into the formation than the larger sizes. This propagation length for the 40/70 sand is approximately 580'. The **Fig. 54** above is a representation of a single cluster within one stage of the reservoir and the fracture is propped with size 30/50 sand. Size 30/50 sand is the larger of the two sands used and doesn't not propagate as far into the formation. This propagation length for the 30/50 sand is approximately 500'. This makes sense because the further from the wellbore the fracture becomes, the smaller the space available for the sand becomes and leads to the smaller sands reaching further into the formation. Both of the simulations in Figure 64 and 65 use the same reservoir and completion characteristics. Most significant are the use of 3,000 lb/ft^2 of sand and 50 bbl/ft^2 of fluid used

with each stage. The limiting factor is the amount of sand used. Comparing the two different fractures, the 30/50 sand has a higher concentration of proppant near the wellbore than the 40/70 sand. The higher concentration is once again due to the size difference between the two and can be seen through the increase of the red hue nearer to the wellbore. The larger sand cannot reach further into the reservoir and results in a higher concentration in the affected areas. The smaller sand has a lower concentration in the affected areas because of the further reach. The concentrations would change dependent on the amount of proppant used but the 3,000 lb/ft^2 of proppant for both sand sizes. When considering the fractures must be propped open with the sand, the importance of the sand becomes clear. The fracture conductivity is dependent upon the type of proppant used and the size of the proppant. A poorly propped fracture will not correlate to the proper fracture conductivity trends from the industry data sets and will generate an inaccurate model for production. Proper fracture modeling and accurate lab measurements for proppant dependent fracture conductivity must be reliable.

The change in fracture permeability has a significant effect on overall production which is clear when modeling the individual cases. These individual models will show how large or small the effect of compaction is on cumulative production. The **Fig. 55** below shows comparatively the 9 runs that were created.

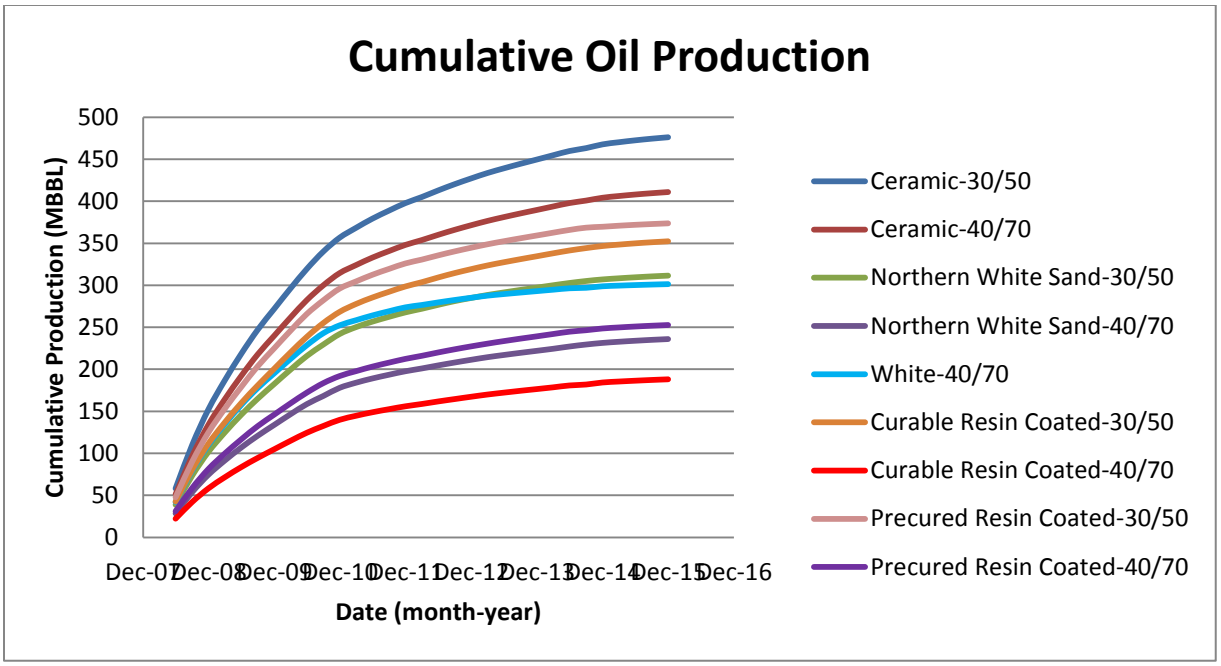

Figure 55: Production of analogous wells

The data was exported from CMG into excel to better compare the final data and to run economics which will be covered in the next section. It is important to note from the graph that the production begins in July of 2008 and ends in December of 2015 which equates to a 7.5 year production cycle. The ceramic-30/50 production line is the blue line at the top and the red line on the bottom is curable resin coated-40/70. At a glance, the production data seems to back up the fracture conductivity tables which makes sense because production will increase with better fracture permeability. What is not representative in the production data is whether or not the individual case is economic. Each of the production trends represents a different proppant used in completion, but each type of sand will have a different cost per pound. Ceramics are the most expensive, which makes sense because they have the best fracture conductivity. Resin coated sands are the next most expensive and the northern white sands are the cheapest which also

correlates to the fracture conductivity table. The **Table 8** compares total cumulative production of the 9 different fracture conductivity scenarios.

Table 8: Analytic Comparison

	Ceramic -30/50	Ceramic -40/70	Northern White Sands-30/50	Northern White Sands-40/70	White-40//70	Curable Resin Coated-30/50	Curable Resin Coated-40/70	Precured Resin Coated-30/50	Precured Resin Coated-40/70
Cum. Prod. (MBBL)	476.132	410.913	311.471	235.960	301.35	352.341	188.080	373.689	252.697

The most productive cases is the ceramic-30/50 case with a total production of approximately 476 MBBL and the least productive case is the curable resin coated-40/70 with a total production of approximately 188 MBBL. There is a total difference of approximately 288 MBBL of total production. There is also a clustering of data for the non-ceramic by size. The different 30/50 sized sands range from 311-373 MBBL and the 40/70 sized sands range from 188-301 MBBL. The clustered data is clear evidence that the larger sand sizes have better total production which makes sense because the larger sand sizes have a higher resistance to crushing. The large differences between the best and worst case and the differences between the 30/50 and 40/70 sands highlight the impact of fracture permeability on total cumulative production. These huge changes in production easily determine the economic viability of a project which will be evident in the next section.

7. ECONOMIC EVALUATION

This final section covers the economic viability of the Wolfcamp Shale formation. Using the field data collected from the analogous well, the reservoir will be analyzed for potential profits. All 9 cases are represented below but 3 of the scenarios will be more scrutinized over the other and they are the ceramic-30/50, northern white sands, and curable resin coated-40/70 scenarios. These were selected for further scrutiny because they represent the most productive, highest Return on Investment and least productive scenarios, respectively. The three represented cases will be evaluated on a yearly base using an average oil price for the years 2008 through 2015 represented in **Table 9** below. A few other metrics represented in Table 9 are the completion stage metrics (amount of proppant used per foot by weight, the amount of fluid used by foot per weight, the length of the lateral, number of stages, number of clusters per stage, and the stage spacing), the overriding royalty interest (ORRI) and the tax on oil in Texas (Pioneer Natural Resources Co., 2018). The completion stage metrics are used for determining the amount of proppant by weight used. The ORRI is the percent paid to the mineral owner from the value of produced fluids and the oil tax is the percent paid to the state of Texas from the value of produced fluids.

Table 9: Oil Price per Year

Year	Oil, $/bbl	Metric		Units
2008	44.6	Proppant	3000	lb/ft
2009	79.36	Fluid	50	lb/ft
2010	91.38	Lateral	10000	ft
2011	98.83	Stages	40	#
2012	91.82	Stage Spacing	240	ft
2013	100.2	Clusters	5	#/stage
2014	90.37	ORRI	17	%
2015	43.41	Texas Oil Tax	4.6	%

The years through 2008 to 2015 were used to correspond with the original history match and the analogous well, as mentioned before, was forecasted 7.5 years out. Using these historical oil prices, the ceramic-30/50 case was analyzed first for economic viability of the Wolfcamp Shale. In **Table 10** below, the yearly liquid production, value of liquids produced, net revenue, the Net Present Value at 10%, and the cash flow of production using a $9,000,000 capital expenditure (CAPEX) and a $4 per barrel operating expenditure (OPEX) are calculated. The CAPEX used is calculated using the completion stage metric and a price of northern white sands at $0.07. The resin coated sand price used is $0.17 and the ceramic sand price used is $0.27, both of which are averages from service company data sheets. This means when calculating the cash flow, the CAPEX has and additive to represent the cost difference in sands which in turn represent the cost difference in obtaining better fracture conductivity.

Table 10: Ceramic-30/50

Ceramic-30/50						
CAPEX=	$ 9,000,000.00	OPEX ($/BBL)=	$ 4.00	Completion ($/LB)=	0.27	
Year	Liquids, MBBL	Value	Net Revenue	NPV10, $MM	Cash Flow	Cum. Cash Flow
2008	152.390	$ 6,796,593	$ 5,328,529.00	$ 6.18	$ (10,041,031)	$ (10,041,031)
2009	119.348	$ 9,471,460	$ 7,425,625.00	$ 8.61	$ 6,948,233	$ (3,092,798)
2010	84.967	$ 7,764,248	$ 6,087,170.36	$ 7.06	$ 5,747,304	$ 2,654,506
2011	41.082	$ 4,060,110	$ 3,183,126.51	$ 3.69	$ 3,018,799	$ 5,673,305
2012	29.393	$ 2,698,852	$ 2,115,900.29	$ 2.45	$ 1,998,329	$ 7,671,634
2013	22.444	$ 2,248,927	$ 1,763,158.67	$ 2.04	$ 1,673,381	$ 9,345,015
2014	18.048	$ 1,630,998	$ 1,278,702.24	$ 1.48	$ 1,206,510	$ 10,551,526
2015	8.460	$ 367,249	$ 287,922.90	$ 0.33	$ 254,083	$ 10,805,608
	Total:	$ 35,038,437	$ 27,470,134.96	$ 31.85	$ 10,805,608	
	Mean:	$ 4,379,805		$ 3.98	$ 1,350,701	

The total monetary value of the produced liquids for the ceramic-30/50 scenario is $35,038,437 and has an NPV of $31,850,000. Considering CAPEX to be approximately $9,000,000, and an additional completion cost of $5,760,000 for ceramics and the OPEX to be about $4/BBL yearly, the ceramic-30/50 case will net approximately $10,805,608. It is important to note that the time to pay out for this scenario is 25 months and continuing the decline trend into 2016 the ceramic-30/50 case will no longer be economic to produce from because the quantity of liquids produced will be too low. The well would need some form of stimulation to become economically viable again.

Table 11: Ceramic-40/70

Ceramic-40/70						
CAPEX=	$ 9,000,000.00	OPEX ($/BBL)=	$ 4.00	Completion ($/LB)=	0.27	
Year	Liquids, MBBL	Value	Net Revenue	NPV10, $MM	Cash Flow	Cum. Cash Flow
2008	134.073	$ 5,979,659	$ 4,688,052.97	$ 5.44	$ (10,608,239)	$ (10,608,239)
2009	105.700	$ 8,388,354	$ 6,576,469.74	$ 7.63	$ 6,153,670	$ (4,454,570)
2010	74.779	$ 6,833,303	$ 5,357,309.42	$ 6.21	$ 5,058,194	$ 603,624
2011	33.459	$ 3,306,726	$ 2,592,472.86	$ 3.01	$ 2,458,638	$ 3,062,262
2012	23.460	$ 2,154,081	$ 1,688,799.80	$ 1.96	$ 1,594,960	$ 4,657,222
2013	18.157	$ 1,819,281	$ 1,426,316.59	$ 1.65	$ 1,353,691	$ 6,010,913
2014	14.546	$ 1,314,565	$ 1,030,619.27	$ 1.20	$ 972,433	$ 6,983,346
2015	6.740	$ 292,575	$ 229,378.58	$ 0.27	$ 202,419	$ 7,185,766
	Total:	$ 30,088,545	$ 23,589,419.23	$ 27.35	$ 7,185,766	
	Mean:	$ 3,761,068		$ 3.42	$ 898,221	

Consider the ceramic-40/70 scenario in **Table 11** above. The total monetary value of the produced liquids for the ceramic-40/70 scenario is $30,088,545and has an NPV of $27,350,000. Considering CAPEX to be approximately $9,000,000, an additional completion cost of $5,760,000 for ceramics and the OPEX to be about $4/BBL yearly, the ceramic-40/70 case will net approximately $7,185,766. The time to pay out for this scenario is about 29 months which is 4 months longer to pay out than the ceramic-30/50 scenario. This makes sense because the established data shows that the 30/50 size fracture conductivity is more productive than the 40/70 size fracture conductivity and the 30/50 would yield a quicker time to payout when comparing similar types.

Table 12: Northern White Sand-30/50

Northern White Sands-30/50						
CAPEX=	$ 9,000,000.00	OPEX ($/BBL)=	$ 4.00	Completion ($/LB)=	0.07	
Year	Liquids, MBBL	Value	Net Revenue	NPV10, $MM	Cash Flow	Cum. Cash Flow
2008	101.797	$ 4,540,124	$ 3,559,457.37	$ 4.13	$ (5,847,729)	$ (5,847,729)
2009	80.572	$ 6,394,190	$ 5,013,045.08	$ 5.81	$ 4,690,757	$ (1,156,971)
2010	59.678	$ 5,453,394	$ 4,275,460.81	$ 4.96	$ 4,036,748	$ 2,879,777
2011	25.696	$ 2,539,561	$ 1,991,015.68	$ 2.31	$ 1,888,231	$ 4,768,007
2012	17.180	$ 1,577,425	$ 1,236,700.93	$ 1.43	$ 1,167,983	$ 5,935,990
2013	12.308	$ 1,233,244	$ 966,863.07	$ 1.12	$ 917,632	$ 6,853,622
2014	9.718	$ 878,218	$ 688,522.88	$ 0.80	$ 649,651	$ 7,503,273
2015	4.522	$ 196,322	$ 153,916.23	$ 0.18	$ 135,826	$ 7,639,099
	Total:	$ 22,812,477	$ 17,884,982.04	$ 20.74	$ 7,639,099	
	Mean:	$ 2,851,560		$ 2.59	$ 954,887	

Consider the northern white sand-30/50 scenario in **Table 12** above. The total monetary value of the produced liquids for the northern white sand-30/50 scenario is $22,812,477 and has an NPV of $20,740,000. Considering CAPEX to be approximately $9,000,000, no additional completion cost because northern white sand is considered in the CAPEX and the OPEX to be about $4/BBL yearly, the northern white sand-30/50 case will net approximately $7,639,099. The time to pay out for this scenario is about 21 months which is 4 months quicker to pay out than the ceramic-30/50 scenario. This does not seem to correlate with the fracture conductivity of the ceramic versus the northern white sand because the fracture permeability trend of the ceramic-30/50 is much greater than that of the northern white sand. This discrepancy will be explained further in the next segment of the research.

Table 13: Northern White Sand-40/70

Northern White Sands-40/70						
CAPEX=	$ 9,000,000.00	OPEX ($/BBL)=	$ 4.00	Completion ($/LB)=	0.07	
Year	Liquids, MBBL	Value	Net Revenue	NPV10, $MM	Cash Flow	Cum. Cash Flow
2008	74.585	$ 3,326,471	$ 2,607,953.13	$ 3.02	$ (6,690,385)	$ (6,690,385)
2009	59.181	$ 4,696,569	$ 3,682,109.88	$ 4.27	$ 3,445,388	$ (3,244,997)
2010	44.231	$ 4,041,859	$ 3,168,817.73	$ 3.67	$ 2,991,892	$ (253,105)
2011	19.673	$ 1,944,310	$ 1,524,338.71	$ 1.77	$ 1,445,646	$ 1,192,541
2012	13.684	$ 1,256,427	$ 985,039.02	$ 1.14	$ 930,305	$ 2,122,845
2013	10.672	$ 1,069,372	$ 838,387.76	$ 0.97	$ 795,698	$ 2,918,544
2014	9.386	$ 848,257	$ 665,033.43	$ 0.77	$ 627,487	$ 3,546,031
2015	4.548	$ 197,407	$ 154,767.07	$ 0.18	$ 136,577	$ 3,682,608
	Total:	$ 17,380,672	$ 13,626,446.73	$ 15.80	$ 3,682,608	
	Mean:	$ 2,172,584		$ 1.98	$ 460,326	

Consider the northern white sand-40/70 scenario in **Table 13** above. The total monetary value of the produced liquids for the northern white sand-40/70 scenario is $17,380,672 and has an NPV of $27,350,000. Considering CAPEX to be approximately $9,000,000, no additional completion cost because northern white sand is considered in the CAPEX and the OPEX to be about $4/BBL yearly, the northern white sand-40/70 case will net approximately $3,682,608. The time to pay out for this scenario is about 32 months which is 11 months longer to pay out than the northern white sand-30/50 scenario. Just like the ceramic scenarios, this makes sense because the established data shows that the 30/50 size fracture conductivity is more productive

than the 40/70 size fracture conductivity and the 30/50 would yield a quicker time to payout when comparing similar types.

Table 14: White-40/70

White-40//70						
CAPEX=	$ 9,000,000.00	OPEX ($/BBL)=	$ 4.00	Completion ($/LB)=	0.07	
Year	Liquids, MBBL	Value	Net Revenue	NPV10, $MM	Cash Flow	Cum. Cash Flow
2008	109.924	$ 4,902,609	$ 3,843,645.58	$ 4.46	$ (5,596,050)	$ (5,596,050)
2009	85.162	$ 6,758,485	$ 5,298,652.11	$ 6.14	$ 4,958,003	$ (638,048)
2010	57.279	$ 5,234,140	$ 4,103,565.52	$ 4.76	$ 3,874,450	$ 3,236,403
2011	21.383	$ 2,113,299	$ 1,656,826.58	$ 1.92	$ 1,571,294	$ 4,807,696
2012	11.417	$ 1,048,312	$ 821,876.29	$ 0.95	$ 776,208	$ 5,583,905
2013	7.861	$ 787,666	$ 617,530.14	$ 0.72	$ 586,086	$ 6,169,991
2014	7.479	$ 675,896	$ 529,902.10	$ 0.61	$ 499,985	$ 6,669,976
2015	2.546	$ 110,519	$ 86,646.80	$ 0.10	$ 76,463	$ 6,746,439
	Total:	$ 21,630,925	$ 16,958,645.13	$ 19.66	$ 6,746,439	
	Mean:	$ 2,703,866		$ 2.46	$ 843,305	

Consider the white sand-40/70 scenario in **Table 14** above. The total monetary value of the produced liquids for the white sand-40/70 scenario is $21,630,925 and has an NPV of $19,660,000. Considering CAPEX to be approximately $9,000,000, no additional completion cost because white sand is considered in the CAPEX and the OPEX to be about $4/BBL yearly, the white sand-40/70 case will net approximately $6,746,439. The time to pay out for this scenario is about 20 months which is 12 months quicker to pay out than the northern white sand-40/70 scenario. This white sand-40/70 fracture conductivity table was used to emphasize the

difference in quality of similar sands. Both northern white sand-40/70 and white sand-40/70 are similar in type and size, however, the white sand-40/70 is of higher quality sand. This higher quality sand yields a better fracture conductivity which, in turn, nets nearly twice as much profit as the northern white sand-40/70. Similarly, because of the better fracture conductivity from the cheaper sand, the time to pay out is the fastest of all the scenarios.

Table 15: Curable Resin Coated-30/50

Curable Resin Coated-30/50						
CAPEX=	$ 9,000,000.00	OPEX ($/BBL)=	$ 4.00	Completion ($/LB)=	0.17	
Year	Liquids, MBBL	Value	Net Revenue	NPV10, $MM	Cash Flow	Cum. Cash Flow
2008	111.549	$ 4,975,106	$ 3,900,483.23	$ 4.52	$ (8,425,715)	$ (8,425,715)
2009	89.007	$ 7,063,613	$ 5,537,872.42	$ 6.42	$ 5,181,844	$ (3,243,871)
2010	67.863	$ 6,201,288	$ 4,861,809.72	$ 5.64	$ 4,590,359	$ 1,346,488
2011	30.150	$ 2,979,736	$ 2,336,113.07	$ 2.71	$ 2,215,513	$ 3,562,001
2012	20.652	$ 1,896,262	$ 1,486,669.59	$ 1.72	$ 1,404,062	$ 4,966,062
2013	15.331	$ 1,536,146	$ 1,204,338.20	$ 1.40	$ 1,143,015	$ 6,109,077
2014	12.135	$ 1,096,669	$ 859,788.63	$ 1.00	$ 811,247	$ 6,920,325
2015	5.653	$ 245,402	$ 192,395.29	$ 0.22	$ 169,783	$ 7,090,108
	Total:	$ 25,994,222	$ 20,379,470.13	$ 23.63	$ 7,090,108	
	Mean:	$ 3,249,278		$ 2.95	$ 886,263	

Consider the curable resin coated-30/50 scenario in **Table 15** above. The total monetary value of the produced liquids for the curable resin coated-30/50 scenario is $25,994,222 and has an NPV of $23,630,000. Considering CAPEX to be approximately $9,000,000, an additional completion cost of $2,880,000 for resin coated and the OPEX to be about $4/BBL yearly, the

curable resin coated-30/50 case will net approximately $7,090,108. The time to pay out for this scenario is about 27 months which is 6 months longer to pay out than the northern white sand-30/50 scenario. Similarly to the northern white sand-30/50 scenario, the curable resin coated-30/50 fracture conductivity trend is greater than the northern white sand-30/50 fracture conductivity trend but has a longer time to pay out. This seems to be counterintuitive to the implication of fracture conductivity and will be further explained in a later section of the research.

Table 16: Curable Resin Coated-40/70

Curable Resin Coated-40/70						
CAPEX=	$ 9,000,000.00	OPEX ($/BBL)=	$ 4.00	Completion ($/LB)=	0.17	
Year	Liquids, MBBL	Value	Net Revenue	NPV10, $MM	Cash Flow	Cum. Cash Flow
2008	58.337	$ 2,601,837	$ 2,039,839.84	$ 2.37	$ (10,073,509)	$ (10,073,509)
2009	46.443	$ 3,685,711	$ 2,889,597.17	$ 3.35	$ 2,703,825	$ (7,369,683)
2010	35.127	$ 3,209,943	$ 2,516,595.05	$ 2.92	$ 2,376,085	$ (4,993,598)
2011	16.072	$ 1,588,428	$ 1,245,327.37	$ 1.44	$ 1,181,038	$ (3,812,560)
2012	11.402	$ 1,046,953	$ 820,811.18	$ 0.95	$ 775,202	$ (3,037,358)
2013	9.109	$ 912,713	$ 715,566.62	$ 0.83	$ 679,131	$ (2,358,227)
2014	7.827	$ 707,354	$ 554,565.68	$ 0.64	$ 523,256	$ (1,834,970)
2015	3.761	$ 163,276	$ 128,008.28	$ 0.15	$ 112,963	$ (1,722,007)
	Total:	$ 13,916,213	$ 10,910,311.18	$ 12.65	$ (1,722,007)	
	Mean:	$ 1,739,527		$ 1.58	$ (215,251)	

Consider the curable resin coated-40/70 scenario in **Table 16** above. The total monetary value of the produced liquids for the curable resin coated-40/70 scenario is $13,916,213 and has

an NPV of $12,650,000. Considering CAPEX to be approximately $9,000,000, an additional completion cost of $2,880,000 for resin coated and the OPEX to be about $4/BBL yearly, the curable resin coated-40/70 case will lose approximately $1,722,007. This scenario does not have a time to pay out because the fracture conductivity trend of curable resin coated-40/70 does not have a large enough effect on production to overcome the effects of ORRI, oil taxes, CAPEX, addition completion costs, and OPEX. This scenario is the only one that never nets a profit which makes sense because of all 9 cases the fracture conductivity trend of curable resin coated-40/70 is the lowest.

Table 17: Precured Resin Coated-30/50

Precured Resin Coated-30/50						
CAPEX=	$ 9,000,000.00	OPEX ($/BBL)=	$ 4.00	Completion ($/LB)=	0.17	
Year	Liquids, MBBL	Value	Net Revenue	NPV10, $MM	Cash Flow	Cum. Cash Flow
2008	124.858	$ 5,568,675	$ 4,365,841.42	$ 5.06	$ (8,013,591)	$ (8,013,591)
2009	99.986	$ 7,934,877	$ 6,220,943.82	$ 7.21	$ 5,821,000	$ (2,192,591)
2010	71.266	$ 6,512,309	$ 5,105,649.94	$ 5.92	$ 4,820,585	$ 2,627,994
2011	29.858	$ 2,950,844	$ 2,313,461.87	$ 2.68	$ 2,194,031	$ 4,822,025
2012	18.734	$ 1,720,140	$ 1,348,589.57	$ 1.56	$ 1,273,654	$ 6,095,679
2013	14.545	$ 1,457,375	$ 1,142,582.02	$ 1.32	$ 1,084,403	$ 7,180,082
2014	10.397	$ 939,579	$ 736,630.05	$ 0.85	$ 695,042	$ 7,875,124
2015	4.045	$ 175,591	$ 137,663.14	$ 0.16	$ 121,483	$ 7,996,608
	Total:	$ 27,259,390	$ 21,371,361.85	$ 24.78	$ 7,996,608	
	Mean:	$ 3,407,424		$ 3.10	$ 999,576	

Consider the precured resin coated-30/50 scenario in **Table 17** above. The total monetary value of the produced liquids for the precured resin coated-30/50 scenario is $27,259,390 and has an NPV of $24,780,000. Considering CAPEX to be approximately $9,000,000, an additional completion cost of $2,880,000 for resin coated and the OPEX to be about $4/BBL yearly, the precured resin coated-30/50 case will net approximately $7,996,608. The time to pay out for this scenario is about 24 months which is 2 months quicker to pay out than the cured resin coated-30/50 scenario. This makes sense because the precured resin coated-30/50 fracture conductivity trend is great than the cured resin coated-30/50 fracture conductivity trend meaning the precured resin coated-30/50 will produce and pay out quicker than the cured resin coated-30/50. However, similarly to the precured resin coated-30/50, the cured resin coated-30/50 scenario does not pay out as quickly as the northern white sands-30/50 scenario despite having a better fracture conductivity trend.

Table 18: Precured Resin Coated-40/70

Precured Resin Coated-40/70						
CAPEX=	$ 9,000,000.00	OPEX ($/BBL)=	$ 4.00	Completion ($/LB)=	0.17	
Year	Liquids, MBBL	Value	Net Revenue	NPV10, $MM	Cash Flow	Cum. Cash Flow
2008	81.365	$ 3,628,877	$ 2,845,039.78	$ 3.30	$ (9,360,420)	$ (9,360,420)
2009	64.630	$ 5,129,027	$ 4,021,157.36	$ 4.66	$ 3,762,638	$ (5,597,782)
2010	46.041	$ 4,207,245	$ 3,298,479.94	$ 3.82	$ 3,114,315	$ (2,483,467)
2011	20.353	$ 2,011,469	$ 1,576,991.88	$ 1.83	$ 1,495,581	$ (987,886)
2012	14.911	$ 1,369,140	$ 1,073,405.68	$ 1.24	$ 1,013,761	$ 25,875
2013	11.953	$ 1,197,663	$ 938,967.61	$ 1.09	$ 891,157	$ 917,031
2014	9.339	$ 843,984	$ 661,683.42	$ 0.77	$ 624,327	$ 1,541,358
2015	4.105	$ 178,192	$ 139,702.59	$ 0.16	$ 123,283	$ 1,664,641
	Total:	$ 18,565,597	$ 14,555,428.26	$ 16.88	$ 1,664,641	
	Mean:	$ 2,320,700		$ 2.11	$ 208,080	

Consider the precured resin coated-40/70 scenario in **Table 18** above. The total monetary value of the produced liquids for the precured resin coated-40/70 scenario is $18,565,597 and has an NPV of $16,880,000. Considering CAPEX to be approximately $9,000,000, an additional completion cost of $2,880,000 for resin coated and the OPEX to be about $4/BBL yearly, the precured resin coated-40/70 case will net approximately $1,664,641. The time to pay out for this scenario is about 54 months which is 30 months longer to pay out than the precured resin coated-30/50 scenario. This makes sense because the precured resin coated-30/50 fracture conductivity trend is great than the precured resin coated-40/70 fracture conductivity trend meaning the precured resin coated-30/50 will produce and pay out quicker than the precured resin coated-

40/70. However, this scenario is barely profitable and takes a significant amount of time to finally net a profit.

A comparative analysis of the 9 different fracture conductivities is difficult to fully comprehend unless represented in a concise table. The 9 scenarios of fracture conductivity related to proppant are all represented in the **Table 19** below which shows the total production, total net profit, the Return on Investment (ROI) and the time to pay out. The ROI is a ratio of the investment to the net revenue and is an important econometric used in evaluating the viability of production scenario. In this research, the 3 econometrics used in evaluating fracture conductivity effects on the viability of the Wolfcamp are the total net profit, the ROI and the time to payout. The first econometric to identify is the total net profit and it is that the majority of the fracture conductivity tables yielded a very profitable simulation. The ceramic-30/50 is the most profitable which makes sense because it has the greatest fracture conductivity. The curable resin coated-40/70 is the least profitable which also makes sense because it has the lowest fracture conductivity. The second econometric to consider is the time to payout which refers to the amount of time it takes for a well to attain a positive net profit. The best time to payout is white-40/70 with 20 months to turn a profit and the worst is the curable resin coated-40/70 which never becomes profitable.

Table 19: Comparative Econometrics

	Cum. Prod. (MBBL)	Net Profit	ROI	Payout, months
Ceramic-30/50	476.132	$ 10,805,608.48	0.648	25
Ceramic-40/70	410.913	$ 7,185,765.56	0.438	29
Northern White Sands-30/50	311.471	$ 7,639,098.87	0.746	21
Northern White Sands-40/70	235.960	$ 3,682,608.07	0.370	32
White-40//70	301.350	$ 6,746,439.37	0.661	20
Curable Resin Coated-30/50	352.341	$ 7,090,107.60	0.534	27
Curable Resin Coated-40/70	188.080	$ (1,722,006.84)	-0.136	-
Precured Resin Coated-30/50	373.689	$ 7,996,607.83	0.598	24
Precured Resin Coated-40/70	252.697	$ 1,664,641.14	0.129	54

The third and most important econometric used is the Return on Investment and is best represented in **Fig. 56** below. The bar graph shows the northern white sands-30/50 scenario as having the highest return on investment which means that per dollar invested the scenario will return an additional $0.746. The worst ROI is from the curable resin coated-40/70 scenario where the Return on Investment is actually -$0.136 which means that the investment is never recovered. This makes sense because as mentioned previously the cured resin coated-40/70 had the worst fracture conductivity and never returned a profit.

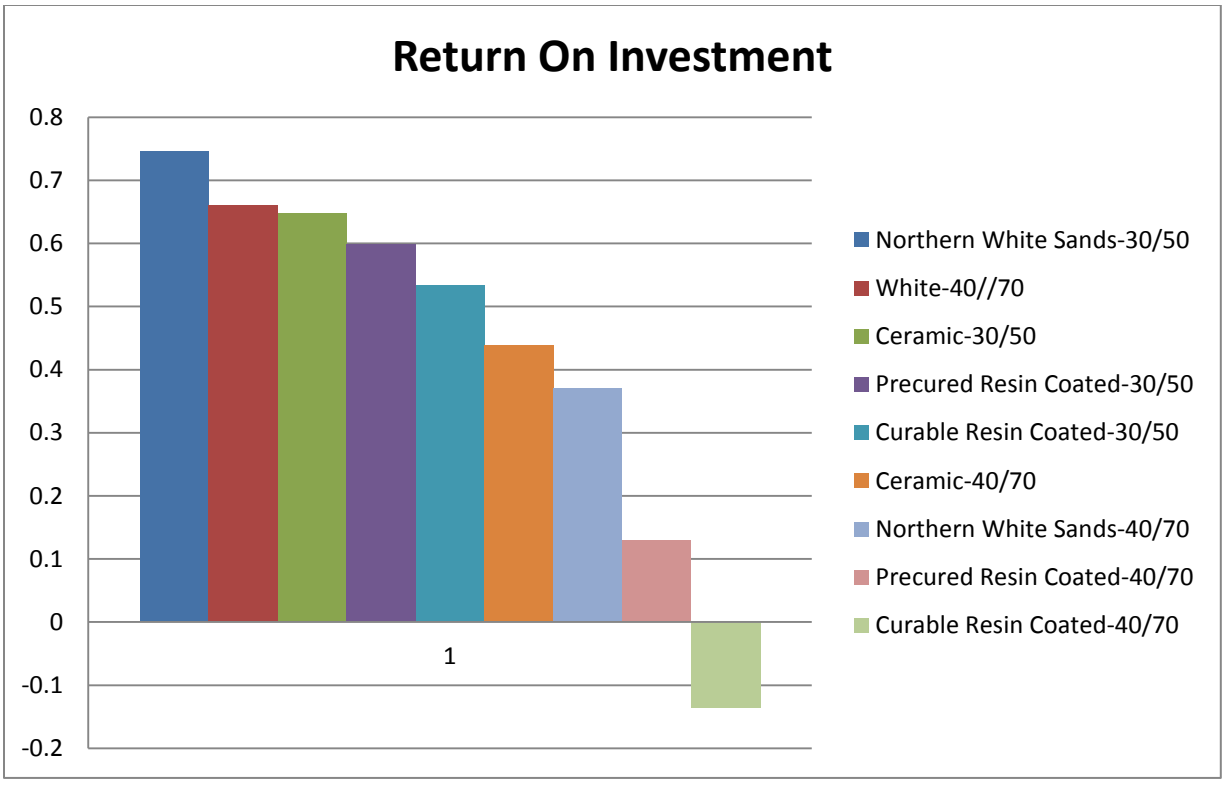

Figure 56: ROI

In the earlier portion of the paper where the 9 cash flow tables are presented, there were a couple of instances that seemed to not compare to the fracture conductivity tables. The problem arises in the additional cost of the proppant respective to the fracture conductivity tables. Both the cured and precured resin coated size 30/50 sands are more resistant to crushing than the norther white sand-30/50 which shows in the better fracture conductivity for the resin. This yields a higher total production which would theoretically yield a higher net profit but this is not the case. Both the northern white sands do not require an additional completion cost because they are accounted for in the CAPEX which was calculated assuming a sand cost of $0.07/lb. The resin coated sands cost approximately $0.17/lb which means an additional completion cost needs to be accounted for with respect to the $0.10 more per pound. This completion cost is enough to

affect both the total net profit and consequently the ROI. Even though better production is yielded for the better fracture conductivity tables, the cost to obtain this better fracture conductivity is not justified in the final economics.

In **Table 20** below, the best two scenarios and the worst scenario are represented. The discrepancy in the resin coatings being accounted for now explains why the northern white sands are the most productive within their relative size clusters. Oppositely, the ceramics are both more expensive and yield a high enough total production to make up for the increased completion cost. The ceramic-30/50 yields the highest total net profit but because of the increased cost for the better fracture conductivity, the ROI is not nearly as high as the northern white sands-30/50. This is due to the relatively cheap cost to use the fracture conductivity table related to the northern white sand-30/50. The approximate $3,000,000 increase between the two scenarios comes at a $5,760,000 cost, which is the reason for the better ROI for northern white sands-30/50. Even though the white-40/70 scenario has a shorter payout time, it is not listed below because the total profit and ROI are much lower than the other two scenarios. Lastly, the worst case is represented below to show the impact of the fracture conductivity on economic viability. Clearly, the fracture conductivity and respective cost of such greatly impact the total profit from a well and highlights the importance of reliable fracture conductivity tables.

Table 20: Notable Scenarios

	Net Cash Flow	ROI	Payout, months
Ceramic-30/50	$ 10,805,608.48	0.648	25
Northern White Sands-30/50	$ 7,639,098.87	0.746	21
Curable Resin Coated-40/70	$ (1,722,006.84)	-0.136	-

These 9 different scenarios are intended to highlight how fracture conductivity affects the economic viability of the Wolfcamp. When considering hydraulic fracturing and the cost of the individual proppants, it is clear that the Wolfcamp is an economically viable reservoir. However, the fracture conductivity table is the most important determining factor in whether or not the well will be profitable. The non-ceramic size 40/70 proppants showcase the importance because they have the lowest fracture conductivity and in turn yield the poorest profits and the non-ceramic size 30/50 have the highest fracture conductivity and in turn yield the higher profits. Technically, some of the non-ceramic size 40/70 sands turn a profit but the low returns mean they are not economically viable. The Wolfcamp is economically viable, but the viability is dependent on the fracture conductivity table used with respect to the cost of the proppant to obtain the necessary fracture conductivity table.

8. CONCLUSION

In the reservoir characterization, the geologic setting of the reservoir is important to not confuse which of the two Wolfcamp formations the data is being sampled from. The range of thickness for Wolfcamp A is 40 to 200 ft., Wolfcamp B is 60 to 400 ft., and Wolfcamp C is 30 to 120 ft. There are also bounding features for the formation, namely the Strawn/Devonian/Ellenburger high-side fault and the Devonian/Ellenburger sub-thrust structure. The OOIP is approximately 23.2 MMSTB however this is just a snapshot of one well within the Wolfcamp, not a study on the full extent of the formation. In the petrophysical evaluation, data preparation was performed in order to correct for environmental effects and depth shift. The cross plot of neutron porosity and bulk density indicated that the matrix density of WB is 2.68 g/cc which are within the range for shale density. To determine shale volume, the sand and shale baseline on the GR log are approximately 12 and 120 API units respectively. Both logs and core porosity data are used to determine porosity of each individual flow unit which showed WA to be 0.10, WB to be 0.26 and WC to be 0.16. The Dual-Water model, Archie's equation along with core data are used to determine the water saturation, which finally shows the water saturation of WA to be 0.75, the WB to be 0.40 and the WC to be 0.60. The permeability is determined from the correlation between core porosity-permeability cross plots and found that WA, WB, and WC are 0.10 md, 688.62 md, and 448.34 respectively. The net sand was determined by implementing cutoffs for the shale volume, water saturation, and porosity. The cutoffs for each variable are determined to be 45 percent, 57 percent, and 19 percent, accordingly. The oil water contact observed is roughly 13,300 feet deep. A table of average petrophysical properties is provided earlier in the report, and a Monte Carlo simulation method was used to account for any

uncertainties in the analysis. In the reservoir performance evaluation, during the pressure transient analysis, the well was modeled as single fault boundary, with correct coefficients including permeability and wellbore storage. The log-log and semi-log plots of pressure transient tests were matched fairly well in both early time build up and history match. The history match for the well production data corresponded very well between the simulation and actual production with only increased error in gas production. Additionally, the well pressure history matched very well between simulation and actual data. Furthering from there, the analogous well simulation forecasted out approximately 8 years for the 9 different scenarios highlighted the effect that proppant dependent fracture conductivity tables have on cumulative production and net profit. The ceramic-30/50 case produced approximately 476,132 barrels of oil over nearly 8 years and the norther white sand-30/50 case produced approximately 311,471 barrels of oil. The ROI of the two best scenarios are 0.648 and 0.746, respectively. The worst case, curable resin coated-40/70, resulted in 188,080 barrels of oil produced which is a significant decrease in production when compared to the other scenarios. The ceramic-30/50 was modeled with the best fracture conductivity table and, as expected, yielded the greatest cumulative production. This case produced enough to overcome the high cost of ceramics and generated the most profit at the expense of a reduced Return on Investment. The northern white sand-30/50 was modeled with the lowest fracture conductivity table of the size 30/50 sands, and yet yielded the highest ROI. This occurred because even though the fracture conductivity for northern white sand-30/50 is not the best for the respective size, the sand is cheap to use compared to the others and results in a better profit when compared to the investment. While 8 of the 9 cases are considered economically viable, the precured resin coated40/70 cases would be a poor choice for investment because of the time to recover CAPEX, low profits, low ROI and short life of the well.

Additionally, the cured resin coated-40/70 is not economic because of the low fracture conductivity and higher cost for resin coated sands. These scenarios make clear the importance of reliable measurements of geomechanical properties, such as the proppant dependent fracture conductivity, and associated modeling such as the proppant filled fractures modeled in FRACPRO. Poor geomechanical properties are represented best by the cured resin coated-40/70 scenario and could potentially create a net loss in profit, when in actuality the same well would be highly productive using a different fracture conductivity table based on a different proppants. Some of the limitations of the methodology used stems from the reliance on the propped fracture conductivity tables. Within the industry, there hundreds of different proppants available and each individual sand correlates to a separate fracture conductivity table. There are a multitude of other sizes of sands but the 30/50 and 40/70 were used because they are prominent in the Wolfcamp. Another limitation is the amount of sand used per stage. The amount of sand will vary dependent on the individual fracture designs for a well. The values used for this economic analysis of the effect of fracture conductivity used field averages. Further analysis into the effect of the fracture conductivity on economic viability of the Wolfcamp would need to consider a larger variety of proppants and a completion design that is tailored to optimize production and not composed of field wide averages. A 10,000' later, with 40 stages composed of 5 clusters spaced with 240' with a proppant and fluid concentration of 3,000 lb/ft^2 and 50 bbl/ft^2, respectively, are all field wide averages. The first recommendation is to put significant effort in the measuring and the modeling of geomechanical properties, such as the proppant dependent fracture conductivity tables and propped fractures. The second recommendation is to continue developing the Wolfcamp formation and to particularly focus on the Wolfcamp B shale layer.

9. REFERENCES

1. *40/70 US Silica White* [Brochure]. (2014) Houston, TX: US Silica.
2. *Atlas Curable Resin Coated-One (CRC-ONE)* [Brochure]. (2016) Berlin, WI: Badger Mining Corporation.
3. *Atlas Precured Resin Coated (PRC)* [Brochure]. (2016) Berlin, WI: Badger Mining Corporation.
4. *Badger Tundra* [Brochure]. (2016) Berlin, WI: Badger Mining Corporation.
5. Barree, R. D., Miskimins, J. L., Conway, M. W., & Duenckel, R. (2016, February 1). Generic Correlations for Proppant Pack Conductivity. Society of Petroleum Engineers. doi:10.2118/179135-MS
6. FRACPRO [Computer software]. (2017). CARBO Ceramics.
7. Gupta, I., Rai, C., Sondergeld, C., & Devegowda, D. (2017, June 17). Rock Typing in Wolfcamp Formation. Society of Petrophysicists and Well-Log Analysts.
8. Kvale, E. P., & Rahman, M. "Wahid." (2016, August 1). Depositional Facies and Organic Content of Upper Wolfcamp Formation (Permian) Delaware Basin and Implications for Sequence Stratigraphy and Hydrocarbon Source. Unconventional Resources Technology Conference. doi:10.15530/URTEC-2016-2457495
9. Lehman, L. (n.d.). [Frac Design]. Unpublished raw data.
10. Malik, M., Schmidt, C., Stockhausen, E. J., Vrubel, N. K., & Schwartz, K. (2013, September 30). Integrated Petrophysical Evaluation of Unconventional Reservoirs in the Delaware Basin. Society of Petroleum Engineers. doi:10.2118/166264-MS

11. NUTECH Energy Alliance Ltd. (2018). *Wolfcamp Fracture Data* [Data File]. Houston, TX: NUTECH Energy Alliance Ltd.
12. Pei, P., He, J., Ge, J., Ling, K., & Qin, W. (2013, August 20). A Correlation to Evaluate the Fracture Permeability Changes as Reservoir is Depleted. Society of Petroleum Engineers. doi:10.2118/165709-MS
13. Pioneer Natural Resources Co. (2018). *Investor Presentation March 2018*. Retrieved from http://investors.pxd.com/static-files/cf1c8bdc-b204-4f42-91af-90e515213d7a.
14. Pioneer Natural Resources Co. (2016). *Well 127 and Formation Data* [Data File]. Irving, TX: Pioneer Natural Resrouces CO.
15. *Proppant Tables* [Brochure]. (2015) Houston, TX: World Oil.
16. Rafatian, N., & Capsan, J. (2015, February 1). Petrophysical Characterization of the Pore Space in Permian Wolfcamp Rocks. Society of Petrophysicists and Well-Log Analysts.
17. Schwartz, K. M., Hennenfent, G., Hegmann, M., Hoffnagle, M., Bain, D., & McCallister, A. (2015, July 20). Pay Distributions and Basin Architecture of the Wolfcamp Shale in the Delaware Basin. Unconventional Resources Technology Conference. doi:10.15530/URTEC-2015 2154738
18. Walls, J. D., Buller, D., Morcote, A., Everts, M. L., & Guzman, B. (2016, August 1). Integration of Whole Core, Drill Cuttings, and Well Log Data for Improved Characterization in the Wolfcamp Formation. Unconventional Resources Technology Conference. doi:10.15530/URTEC-2016-2461526
19. Walls, J. D, & Morcote, A. (2015, July 20). Quantifying Variability of Reservoir Properties From a Wolfcamp Formation Core. Unconventional Resources Technology Conference. doi:10.15530/URTEC-2015-2154633

20. Walls, J. D, Ver Hoeve, M., Morcote, A., & Foster, M. (2017, July 24). Integrated Multi-Scale Reservoir Characterization: Wolfcamp Formation - Midland Basin. Unconventional Resources Technology Conference. doi:10.15530/URTEC-2017-2670796
21. Zanganeh, B., et al. "The Role of Hydraulic Fracture Geometry and Conductivity Profile, Unpropped Zone Conductivity and Fracturing Fluid Flowback on Production Performance of Shale Oil Wells." *Journal of Unconventional Oil and Gas Resources,* Elsevier, 9 Jan. 2015, www.sciencedirect.com/science/article/pii/S221339761400055X.
22. Zhao, Shan, et al. "Thickness, Porosity, and Permeability Prediction: Comparative Studies and Application of the Geostatistical Modeling in an Oil Field." Environmental Systems Research, vol. 3, no. 1, 2014, p. 7. doi:10.1186/2193-2697-3-7.